ISSN. Application No. 21794

Journal of Construction Engineering and Technology

Volume No. 11

Issue No. 1

January - April 2023

ENRICHED PUBLICATIONS PVT. LTD

S-9, IInd FLOOR, MLU POCKET,
MANISH ABHINAV PLAZA-II, ABOVE FEDERAL BANK,
PLOT NO-5, SECTOR-5, DWARKA, NEW DELHI, INDIA-110075,
PHONE: - + (91)-(11)-47026006

ISSN. Application No. 21794

Journal of Construction Engineering and Technology

Aims and Scope

Journal of Construction Engineering, and Technology is focused towards the rapid publication of fundamental research papers on all areas of Construction Engineering, **Focus and Scope Covers**

- Planning and Management of the Construction of Structures
- Design of Temporary Structures
- Quality Assurance and Quality Control
- Building and Site Layout Surveys
- On Site Material Testing,
- Safety Engineering, Materials Procurement, Budgeting & Cost Engineering
- Concrete Mix Design

ISSN. Application No. 21794

Journal of Construction Engineering and Technology

ISSN. Application No. 21794

Journal of Construction Engineering and Technology

(Volume No. 11, Issue No. 1, January - April 2023)

Contents

ISSN. Application No. 21794

Creep Test and Development of Kelvin's Model for Green Pea Kernels Subjected to Uniaxial Compressive Loading

[1]Mohan Singh, [2]Aradhana Patel
[1,2]Department of Post Harvest Process & Food Engineering College of Agricultural Engineering, JNKVV, Jabalpur, India.

ABSTRACT

If a constant load is applied to biological materials and if stresses are relatively large, the material will continue to deform with time, this deformation is known as creep. The objective of this study was to develop a device to facilitate the study of creep behavior of biological materials and to validate the Kelvin model for green pea kernels.

A rectangular wooden box provided with a cylinder cavity to firmly hold the PVC cylinder at the bottom. A stand was provided to facilitate mounting of scale for measurement of downward movement of cover plate inside the cylinder. Two perforated SS plates were used in this experiment. Seven different compressive stresses 177.11, 265.66, 354.22, 442.77, 531.33 and 708.44 N/m2 were used and deformation was observed at different time intervals 0, 0+, 5, 10, 15, 20, 45, 60, 90, 120 and 150 minutes. Creep curves were plotted to show the variation in volumetric strain for different time intervals. The volumetric strain with respect to variation of loading is maximum in case of maximum stress that was 708.44 N/m2. The graphical method was used to develop Kelvin model.

Keywords: rheological behavior, Green Pea Kernels, Compressive loads, Kelvin model.

INTRODUCTION

Static uniaxial normal creep (13) is a condition in which the constant shear or dynamic forces involved are all parallel to the longitudinal axis of the specimen. In the creep experiment, when the load (force) is applied to the sample instantaneously the sample is rapidly deformed, imposing a strain on the material which continues to increase at a decreasing rate as a function of time (12). Regardless of sample dimensions, when the specimen is deformed in compression the strain generated will decrease height of the sample,and result in a increase in the sample diameter or width to a value dependent on the bulk modulus of the material or its poisons ratio (14). In many cases the transverse strain may be neglected because of the partly compressible nature of the most agricultural materials which cause the resultant lateral strain to be negligible when compared to the uniaxial/longitudinal strain (16). A plot of uniaxial strain or deformation as a functions of time results in a curve know as creep curve (13). The creep test can be used to predict the deformation of agricultural products such as fruits, vegetables, silage etc. under dead load as a function of time. This is particularly important for transportation and storage of perishable agricultural products.

Viscoelasticity is the property (1, 10, 13) of materials by the virtue of which it exhibit both viscous (8) and elastic (6) characteristics when undergoing deformation. Food show both viscous and elastic properties which are known as viscoelastic materials. Immediate deformation under load in a biological materials is due to their elastic nature where as the deformation that continuous with time is due to the viscous flow of inter cellular fluids under pressure with time (2, 4, 9).

Creep

If a constant load is applied to biological materials and if stresses are relatively large, the material will continue to deform with time. This slow and progressive deformation with time under a constant stress (15) is known as creep. Creep compliance function is a measure of deformation in a given viscoelastic / biological materials with time (12). It explains how the viscous flow will take place in the viscoelastic materials over the time. In this context the present study is undertaken with following objective:

- To develop a device to facilitate the study of creep behavior of biological materials.
- To validate the Kelvin model for green pea kernels.

MATERIALAND METHODS

Following conceptual drawing was prepared to provide guideline for fabricating equipment for creep test of green pea kernels.

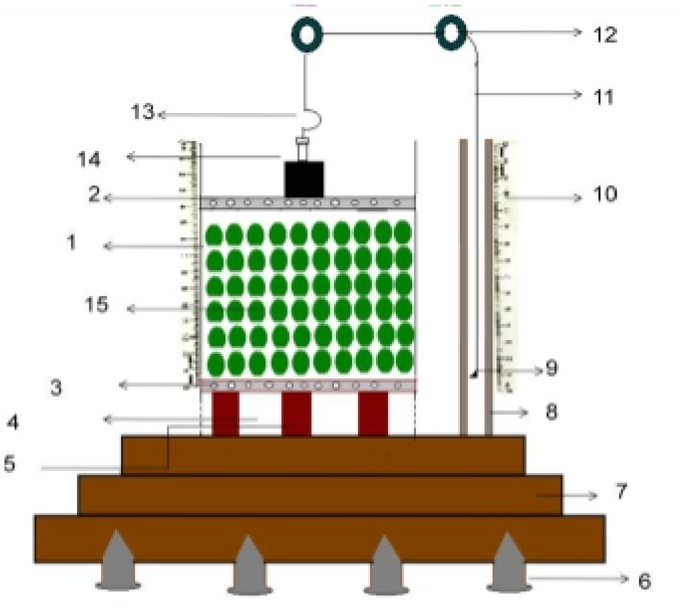

Plate 1 Conceptual drawing of creep test set-up

S. No.	Component	S. No.	Component
1	cylinder	9	Pointer
2	SS upper plate	10	Scale
3	SS lower plate	11	String
4	Plenum chamber	12	Pully
5	Pieces of wood	13	Hook
6	Adjustable screw	14	Weight
7	Wooden support	15	Biological material
8	Guide rail for pointer		

Keeping in mind the above conceptual drawing experimental set-up (plate 2) was fabricated, for determination of creep behavior (5) as well as volumetric strain of biological materials. The equipment consisted of a PVC cylinder 16.6 cm internal diameter and 28 cm in depth and 7 mm thickness of wall was used. This cylinder is used to facilitate placing the grain for uniaxial compressive loading. A rectangular wooden box provided with a cylinder cavity to firmly hold the PVC cylinder at the bottom. There were four adjustable screws attached to the lower part of rectangular wooden box so as to facility alignment with thehorizontal on any platform such that the compressive load applied is perfectly vertical during experimentation. A stand was provided to facilitate mounting of scale for measurement of downward movement of cover plate inside the cylinder. The load applied to the green pea kernels (17) through cover plate placed inside the cylinder was attached to a pointer through a string passing over the four pulleys fitted on the stand.

Plate 2 Experimental set-up

To ensure upward movement of pointer on scale along with the downward movement of load inside the cylinder, the string was attached to a magnet force-fitted through a cap and a hook to the string attached with the pointer. The magnet was attached to the iron load to ensure that the string moves downward inside the cylinder along with the load placed on cover plate. The compression in the green pea kernels resulted in upward movement of pointer attached to the stand. The distance travelled by load inside the cylinder can be directly noted by noting the position of pointer on scale for any given time interval. The PVC cylinder was perforated at the bottom and just above the perforation a perforated SS plate having 16 cm diameter was fitted with the help of four screws threaded at four diametrically opposite position on a horizontal plane just above the perforation. The purpose of lower circular plate is to provide a firm base to hold the green pea kernels inside the cylinder. The bottom plate was provided with perforation so that the respiration of green pea kernels is not obstructed. A similar circular perforated cover plate was provided to cover the green pea kernels on the topand to facilitate placing the desired load on the top surface as well as to transmit the load uniformly over the entire cross section of green pea kernels placed inside the cylinder.

The top cover plate was also perforated to permit the respiration of green pea kernels subjected to compressive loading inside the cylinder. The size of perforation was kept smaller than the smallest green pea kernels used in experimentation.

Green pea kernels:

In this experiment it was decided to use green pea kernels for uniaxial compressive loading. The green pea kernels are usually spherical in shape not so firm yet strong enough to bear large compression without any failure due to surface rupture because the green pea kernels are very flexible in nature (3) therefore elastic component denoted by spring in Kelvin model is comparatively high as compare to any other biomaterial. Also looking to the short season the green pea kernels are depodded stored, processed and again store in small containers. Thus providing a opportunity to investigate the depth of container for long term storage of green pea kernels. In this experiment green pea (irrespective of variety) was purchase from local market. Green pea pod was manually de-podded and used for the experiment.

Methodology

In this experiment seven stresses applied were 177.11, 265.66, 354.22, 442.77, 531.33 and 708.44 N/m2. A sample of green pea kernels weighed in a balance to determine the mass were placed in the cylinder which was shaken to let the kernels settle. These kernels were covered with the cover plate. The depth of the cover plate was measured from the top of the cylinder just before and after the application of load at the four previously marked (diametrically opposite) point on the cylinder. The average of these four readings was used to represent the depth of the cover plate. This depth plus the thickness of the cover plate, when subtracted from the total depth of the cylinder gave the height of the sample present in the cylinder. PVC cylinder had cross sectional area 0.006 m2. The volume of the sample was calculated for each time interval 0+, 5, 10, 15, 20, 45, 60, 90, 120,150 minutes, (0+ is time just after applying the load). The change in volume (ΔV) of the cylinder, at all time interval (0+, 5, 10, 15, 20, 45, 60, 90, 120,150 minutes) with respect to its original volume (V0) was alsocalculated. Knowing the change in volume (ΔV) the corresponding volumetric strain may be calculated.

RESULT AND DISSICUTION

Volumetric strainThe relationship between volumetric strain and duration of loading for the compressive stress of 177.11, 265.66, 354.22, 442.77, 531.33 and 708.44N/m2 is shown in Fig. 1.

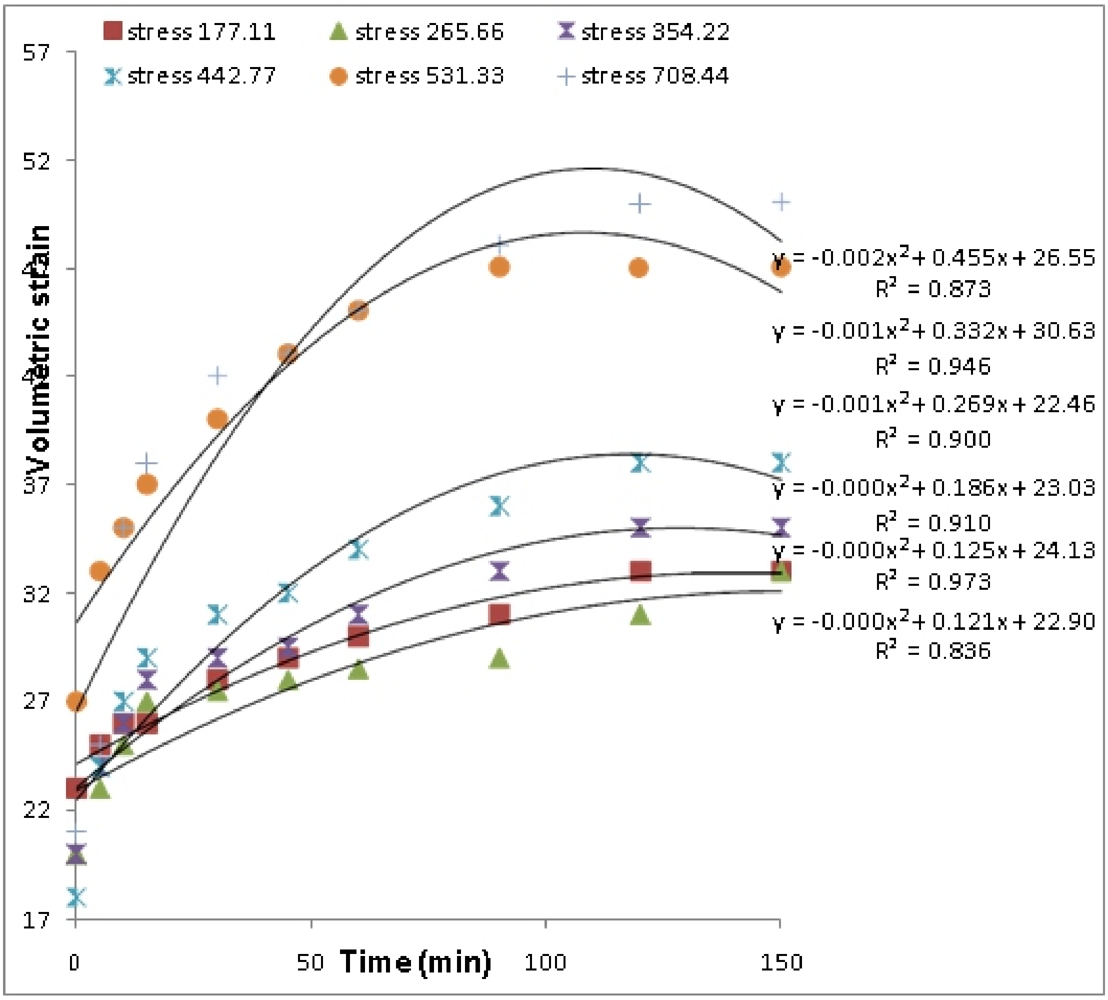

Fig. 1 Curve between volumetric strain and time

From the curve it is evident that the slope of curve is steep at the beginning and then with the increase in duration of loading the slope of curve flattened down which shows that the rate of change of volumetric strain for a given sample at a given stress is large at the beginning and as the time passes, the rate of change becomes less and less. Also as it is noted from the high value of coefficient of deformation (R2 =0.972) the relationship between two variables i. e. change in volumetric strain with respect to time is strongly correlated with each other. The reason for slope of curve being steep initially may be as the load is applied, the seeds getrearrange and the air voids are minimized also the elastic deformation take place only initially. During later part of stress application the slope of curve flattened down, the reason for the slope to flatten down with time may be due to reduction of air voids and because viscoelastic deformation becomes smaller with increase in time. The equation for the Kelvin model (11) for bio materials subjected to compressive load is given by :-

$$\varepsilon = \frac{\sigma_0}{E} + \varepsilon_0 - \frac{\sigma_0}{E} \cdot e^{\frac{-t}{\tau_{ret}}}$$

Where,

ε= strain at time t, ε_0 =initial strain, σ_0 = constant stress,

E = young modulus, t= time, τ_{ret} = retardation time.

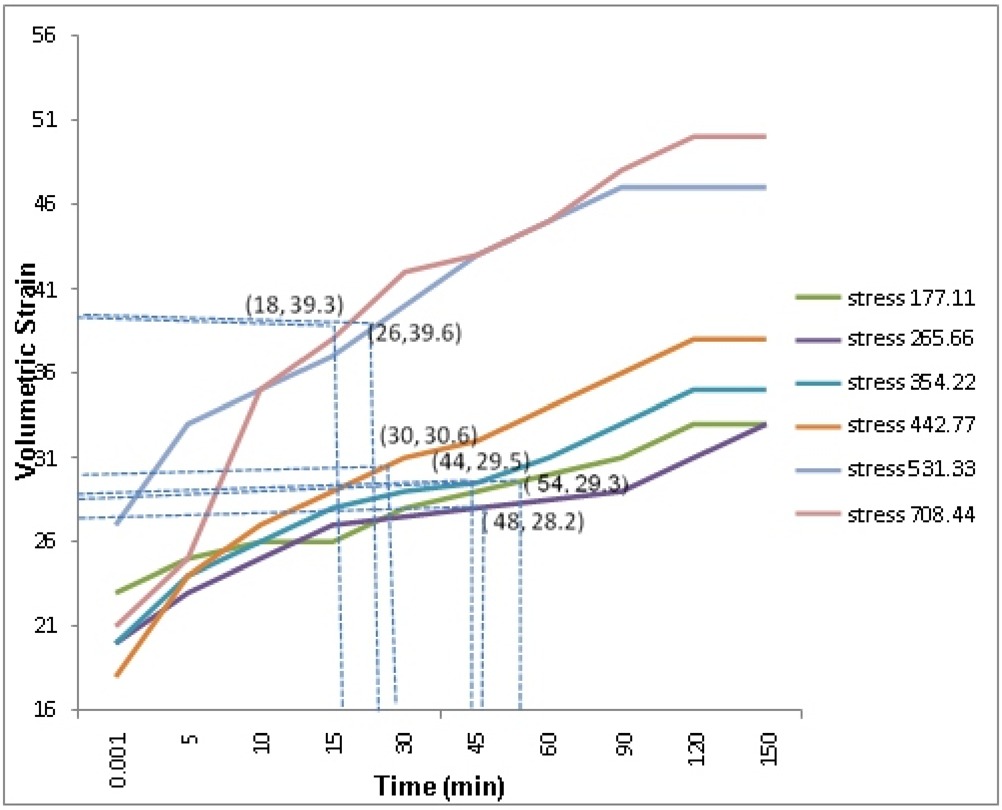

Fig 2 curve between volumetric strain and time

Now as seen from (Fig. 2) the volumetric strain increases with time of application of compressive stress. A tangent to the creep curve drawn from the constant volumetric strainon Y axis gives the value of $\frac{\sigma_0}{E}$ as "33". Also as seen from initial strain at time 0+ that is just after the application of load the volumetric strain is 23. According to the definition the retardation time corresponds to the volumetric strain equal to sum of initial volumetric strain and 63% of difference of ε_0 and $\frac{\sigma_0}{E}$ hich is "10 minute". Therefore the retardation time will converted (7) to the volumetric strain value of 23+63% of 10 =29.3. As noted from graph the retardation time corresponding to volumetric strain of 29.3 is 54 Putting all the values in equation the Kelvin model obtained for compressive loading of green pea kernels for stress of 177.11 N/m2 is

$$\varepsilon_{(177.11)} = 33 - 10.\, e^{\frac{-t}{54}}$$

From the above equation it is noted that for compressive stress of 177.11 N/m2 the retarded deformation starts 54 minute after the application of the stress. During retarded deformation due to spring component becomes insignificant as compared to the retardation due to viscous flow in biomaterials.

Similarly proceeding with the graphical method the Kelvin model was developed for all the remaining five stresses namely 265.66, 354.22, 442.77, 531.33 and 708.44 N/m2, The Kelvin model derived for all the six compressive stresses is tabulated in table 1.

Table 1 Kelvin model with respect to different stresses.

S. No.	Stress N/m2	Kelvin model	Retardation Time
1	177.11	$\varepsilon_{(177.11)} = 33 - 10\,.\, e^{\frac{-t}{54}}$	54
2	265.66	$\varepsilon_{(265.66)} = 33 - 13\,.\, e^{\frac{-t}{48}}$	48
3	354.22	$\varepsilon_{(354.22)} = 35 - 15\,.\, e^{\frac{-t}{44}}$	44
4	442.77	$\varepsilon_{(442.77)} = 38 - 20\,.\, e^{\frac{-t}{30}}$	30
5	531.33	$\varepsilon_{(531.33)} = 47 - 20\,.\, e^{\frac{-t}{26}}$	26
6	708.44	$\varepsilon_{(708.44)} = 50 - 29\,.\, e^{\frac{-t}{18}}$	18

As seen from column no. 4 of table 1 the retardation time decreases with increase in compressive stress. It is noted that the maximum retardation time of 54 seconds corresponds to minimum compressive stress of 177.11 N/m2, whereas the minimum retardation time of 18 seconds corresponds to the maximum compressive stress of 708.44 N/m2. Also as seen from fig. 3 the decrease in retardation time follows a straight line relationship with negative correlated coefficient with decreasing compressive stress. The straight line relationship is given by:

$$Y = -0.0719x + 66.4$$

The negative correlated coefficient value of ($R^2 = 0.957$) shows a strong association between retardation time and compressive stress.

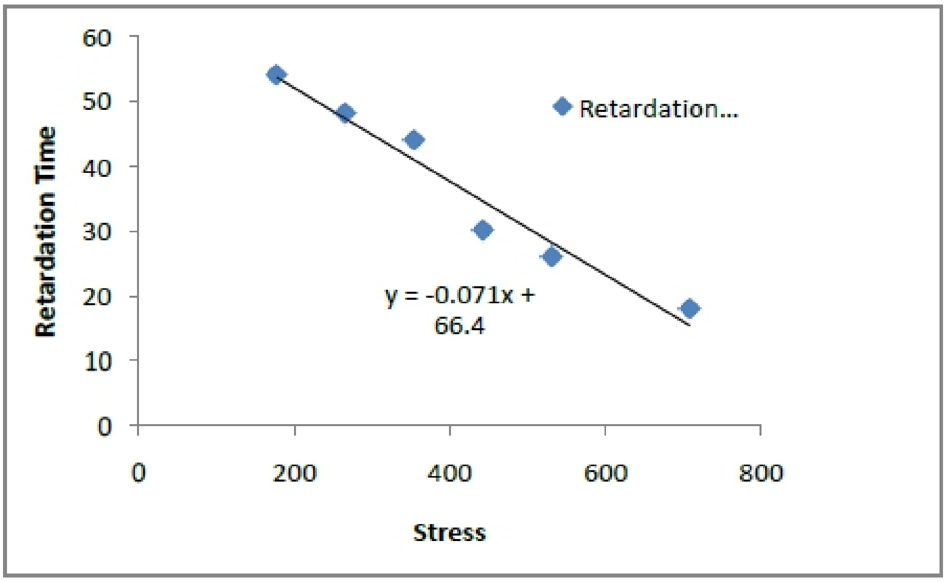

Fig. 3 Variation in time of retardation with different compressive stresses

The decrease in retardation time with increase in compressive stress may be because for higher value of compressive stresses, the elastic phase of deformation in green pea kernels reduces faster as compared to that for smaller value of compressive stress which means for higher compressive stresses the viscous phase in deformation of green pea kernels starts earlier.

CONCLUSION

1. A device as shown in plate no. (1) and (2) was developed for creep test of biological materials. The developed device has a facility for application of different stresses, measurement of volumetric deformation, housing the desired sample in required quantity and for horizontally leveling of device.
2. The developed device is used for measurement of variation in volumetric strain with time for six different stresses namely 177.11, 265.66, 354.22, 442.77, 531.33 and 708.44 N/m2.

The Kelvin model developed for different stresses is tabulated in table (1). It was noted from the Kelvin models the retardation time decreased from 54 minutes for 177.11 N/m2 to 18 minutes for 708.44 N/m2 and decrease in retardation time is found to have a straight line relationship with a strong but negative correlation coefficient.

REFERENCES

1. *Alvarez MD, Canet W, Cuesta F and Lamua, M. 1998. Viscoelastic characterization of solid foods from creep compliance data: Application to potato tissue. Zlebensm Unters Forsch, A, 207: 356–362.*
2. *Ayman H, Amer Eissa, Abdul Rahman O, Alghannam and Mostafa M Azam. 2012. Mathematical Evaluation Changes in Rheological and Mechanical Properties of Pears during Storage under Variable Conditions. Journal of Food Science and Engineering (2): 564-575.*
3. *Banks HT, Hu S and Kenz ZR. 2010. A brief Review of Elasticity and Viscoelasticity for Solids Advances in Applied Mathematics and Mechanics 3(1): 1-51*
4. *Brodt M, Cook LS and Lakes RS. 1995. Apparatus for measuring viscoelastic properties over ten decades: refinements. Review of Scientific Instruments 66(11): 5292-5297.*
5. *Chen CP and Lakes RS. 1989. Apparatus for determining the viscoelastic properties of materials over ten decades of frequency and time. Journal of Rheology 33: 1231-1249.*
6. *Finney,FE and Hall CW. 1967. Elastic properties of potatoes. Transactions of ASAE 10(1): 4-8.*
7. *Kakar R. 2013. rheological responses of viscoelastic models under dynamical loading. European Scientific Journal 9(12): 287-308.*
8. *Kopac M.1999. Evaluation of a Modifed Jefeys Type Model for Viscoelastic Fluids. Tr. J. of Engineering and Environmental Science 23: 49-57.*
9. *Kucharova M, Doubal S, Klemera P, Rejchrt P, Navratil M. 2007. Viscoelasticity of Biological Materials – Measurement and Practical Impact on Biomedicine. Physiol. Res. 56 (1): 33-37.*
10. *Kuo M-I, Wang Y-C, and Gunasekaran S. 2000. A Viscoelasticity Index for Cheese Meltability Evaluation. Journal of Dairy Science 83(3): 412-417.*
11. *Linn J, Lang H and Tuganov A. 2013. Derivation of a viscoelastic constitutive model of Kelvin{Voigt type for Cosserat rods. Berichte des Fraunhofer ITWM, Nr. p225.*
12. *Mainardi F and Spada G. 2011. Creep, Relaxation and Viscosity Properties for Basic Fractional Models in Rheology. The European Physical Journal 193: 133–160.*
13. *Mohsenin NN. 1996. Physical properties of plant and animal materials. Gordon and Breach science publishers,New York p498.*
14. *Raymundoa A, Fradinhob P and Nunesa MC. 2014. Effect of Psyllium Fibre Content on the Textural and Rheological Characteristics of Biscuit and Biscuit Dugh. Bioactive Carbohydrates and Dietary Fibre 3: 96-10*
15. *Suter M and Benipal GS. 2007. Time-Dependent Behaviour of Reacting Viscoelastic Concrete. Latin American Journal of Solids and Structures 4: 103-120.*
16. *Telis VRN, Telis-Romero J and Gabas, AL. 2005. Solids Rheology for Dehydrated Food and Biological Materials. Drying Technology, 23(4): 759-780.*
17. *Zoerb GC. 1967. Instrumentation and measurement Techniques for determination of Physical Properties of agricultural Products. Trans. Of the ASAE 10(1): 100-109.*

ISSN. Application No. 21794

Analysis of Manufacturing of Railways Bogies Through Quality Control Tools

Nitesh Kumar[*], D. R. Prajapati[**]
[*] PG student, Department of Mechanical Engineering,Punjab Engineering College (Deemed to be University), Chandigarh
[**] Professor, Department of Mechanical Engineering,Punjab Engineering College (Deemed to be University), Chandigarh

A B S T R A C T

It is very important improve and maintain the quality of manufactured products now a days to survive in global or local market. Some quality control tools have been applied to one of the leading coach manufacturing industry, located in norther India. The Pare to chart, Fishbone diagram etc. have been applied to find the root causes of failures of components and improving the quality of manufacturing products. It has been established that the organization has numerous issues particularly in dismissal and modifications in the assembly lines. Various processes like CNC cutting, welding, machining, assembly of parts are involved, where probability of defects are more and improvement is required. Pareto chart shows that fault in control arms accounted for 35.3%, while Ankerlink block accounts for 29.35% and gap between pair of control arms are approximately 19%.

Keywords: Quality Control Tools, Pareto chart, Cause & Effect Diagram., Railways coach manufacturing

1. INTRODUCTION

The latest challenge in the current worldwide market is an issue converting into a huge requirement for the proceeding with advancement of the manufacturing. Consequently, world business is ceaselessly in scan for the aggressive edge because of the developing requests of client needs and desires. Quality has a significant job in the business procedure over the whole association, to be increasingly proficient and viable in the worldwide market, in this way improving profitability and client dedication just as increment piece of the overall industry. It isn't just important to decrease the wastage, yet additionally to fulfil client's desires, cost decreases and constant upgrades to get by in profoundly focused condition. Quality improvement is an essential prerequisite in any production framework that sends items or administration as its yields. Hence, it is a noteworthy objective in any assembling and manufacturing industry. Assembling and manufacturing industries spend a great deal of end eavours in keeping up and improving quality of their items utilizing an assortment of quality control tools and methods.

Quality control tools can be connected in item improvement, generation and showcasing additionally. Quality concerns influence the whole association in each aggressive condition. It isn't just important to decrease the wastage, yet in addition to fulfil client's desires, nonstop cost decreases and ceaseless enhancements to make due in exceedingly aggressive condition. The quality control is meant to fulfil the clients by conveyance of imperfection free items. The exploration is meant to research the fruitful Implementation of quality control tools and Techniques in assembling and manufacturing industry. Figure 1 shows the Quality control flow chart.

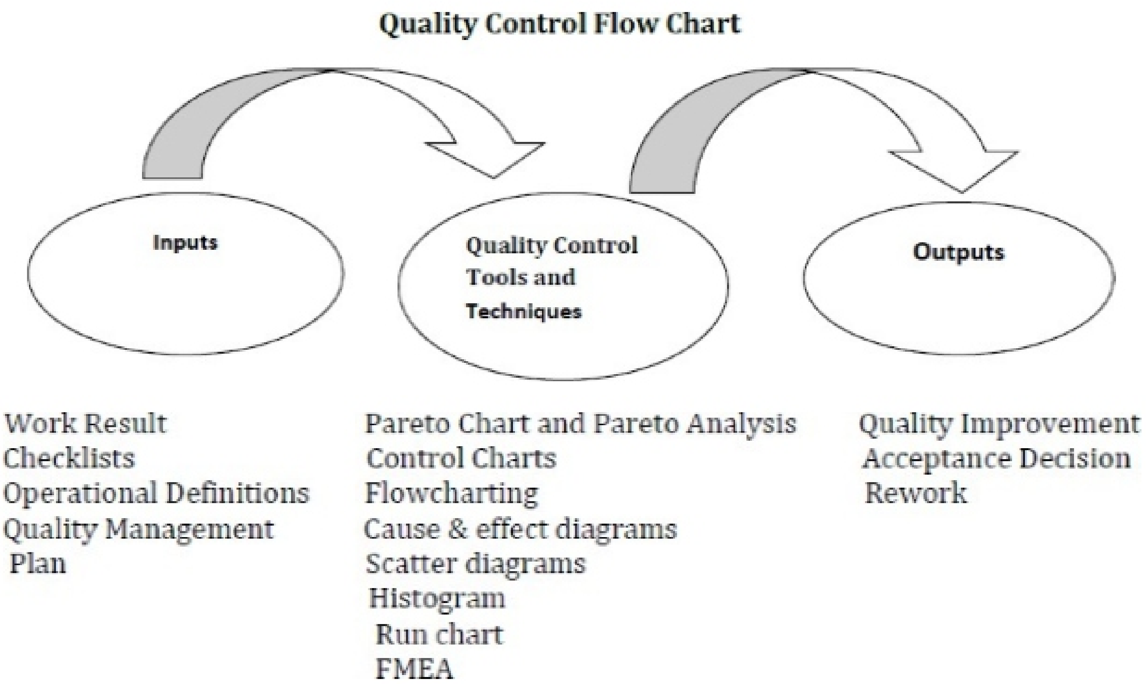

Fig.1 Quality Control Flow Chart

The use of Quality control tools is significant, as it could improve process execution by diminishing item fluctuation and improve generation effectiveness by diminishing scarp and modify. These tools are helpful in (i) Minimization of the dismissal (ii) Enhance consumer loyalty by decrease in client complaints. (iii) Beneficial for decreasing the generation cost (iv) Finding the underlying drivers of issue and improving production execution.

1.1 Quality control tools and techniques

By understands the processes with the goal that they can be improved by methods for an orderly methodology requires the learning of a straightforward pack of tools or methods. The viable utilization of these tools and methods requires their application by the general people who really deal with the procedures, and their responsibility to increase quality may be achievable and guaranteed that the executives thinks about improving quality. The tools and procedures most normally utilized in procedure improvement are:

(I) Process flowcharting (ii) Cause and Effect diagram (iii) Brainstorming (iv) Pareto investigation (v) Control Charts (vi) Check sheets (vii) Scatter graphs (viii) Histograms and (ix) Failure Mode Effect Analysis (FMEA) These tools are very common and popular, so details of these tools are not required in this paper.

2. LITERATURE REVIEW

Gaafar and Keats (1984)focused on the Statistical Process Control (SPC) implementation phase in an effort to underline that SPC is not just control charts, and that many steps have to be accomplished before these charts are used. In addition, they highlighted the role of training and presented it as an ongoing process which involves everyone in the organization. Chan et al.

(2003) contemplated consolidating the consequence of two charts to be specific x-diagramand x- bar graph. Control charts assumed a significant job in observing the presentation of activity forms, as far back as their development.

Saniga et al. (2006)looked at the expenses of a monetarily planned CUSUM control diagram and a typical Shewhart control charts, the X–bar graph for some setups of parameters. They found that there are recognizable locales where X–bar graph can be utilized with no considerable monetary weakness. Prajapati and Mahapatra (2007)examined an extremely straightforward and powerful structure of proposed X-bar and R charts to screen the procedure mean and standard deviation. The idea of the proposed charts depends on the aggregate of chi-square (χ^2) to register and analyze Average Run Lengths (ARLs). They compared their proposed charts with VSS, VSI and VSSI joint plans proposed by Costa (1999).

Fricker (2009) portrayed a system for advancing the Shewhart x-diagram working on parallel creation lines in a production line. They utilized non-direct programming to suitably set the diagram control limits which consolidates the data about the likelihood of every generation line leaving control. By utilizing this methodology, production lines can set their control frameworks to ideally recognize crazy conditions. The objective is to expand the production line wide likelihood of recognizing a crazy condition exposed to a requirement on the normal number. Das and Sachan (2013) discussed the importance of control charts in detecting the assignable cause of variation. They discussed the assumption under which these charts are developed. They proposed some alternatives control charts for controlling location parameters based on some robust estimators, because the present charts are not used with assumption in real situations. Prajapati and Singh (2014) processed ARLs (normal run length) at different arrangements of parameters of the X diagram by reproduction, utilizing MATLAB. The presentation of the graph is estimated as far as the normal run length (ARL), which is the normal number of tests before getting a crazy sign. They made an endeavor to counter autocorrelation by planning the X charts utilizing cautioning limits. They proposed different ideal plans for various dimension of connection.

Singh and Prajapati (2016) examined that both management and employees in the service sector can take advantage of SPC techniques to analyse processes and procedures. Processes may be streamlined to save employee hours. Procedures that lead to mistakes may be changed so that the incidence of mistakes is reduced or eliminated. Employee involvement in the use of charts and check sheets can lead to valuable input in improving the service. It is found from the Pare to analysis that maximum percentage of rejection (33.75%) is due to drive shaft run-outs defects. Other two important causes are Crank shaft bearing diameter undersize & oversize (14.61%) and under size of cylinder block depth (13.28%) respectively. Everard and Hardjono (2018)states In quality administration four standards can be observed: the Empirical, the Reference, the Reflective and the Emergence Paradigm. Right now the Emergence Paradigm is the least created. Following the Emergence Paradigm would mean the fuse of frameworks thinking in initiative preparing, quality administration hypothesis and practices. Rehearsing quality administration from the Emergence Paradigm would embroil for an association to be available to change and its specific circumstance.

Chen et al. (2014) examined that first attempt at developing yield based PCIs for non normal processes. In the literature, the use of classical PCIs such as Cp and Cpk is based on the normality assumption of the process characteristic X. If X is non normal, the percentile-based PCIs cannot quantify the process yield, which limits their usefulness in various applications such as the supplier-selection problem. On the contrary, our proposed PCIs degenerate to the classical PCIs when X is normally distributed, and they have the same quantitative interpretation to the process capability

3.0 INDUSTRY AND PROCESSES

This rail coach factory was laid on 17th August 1985 in the northern part of India and was a timely step towards making good shortfall and complementing the coach manufacturing capacity of Railway's other manufacturing units. The present production capacity of this plant is approximately 2000 coaches per year. Various kinds of coaches- AC, Non-AC, Chair Car, Tejas, MG Diesel Electrical Multiple Units, Main Line Electrical Multiple Units etc. are manufactured in this plant of India. Flow process chart for manufacturing of railways bogies is shown in Figure 2.

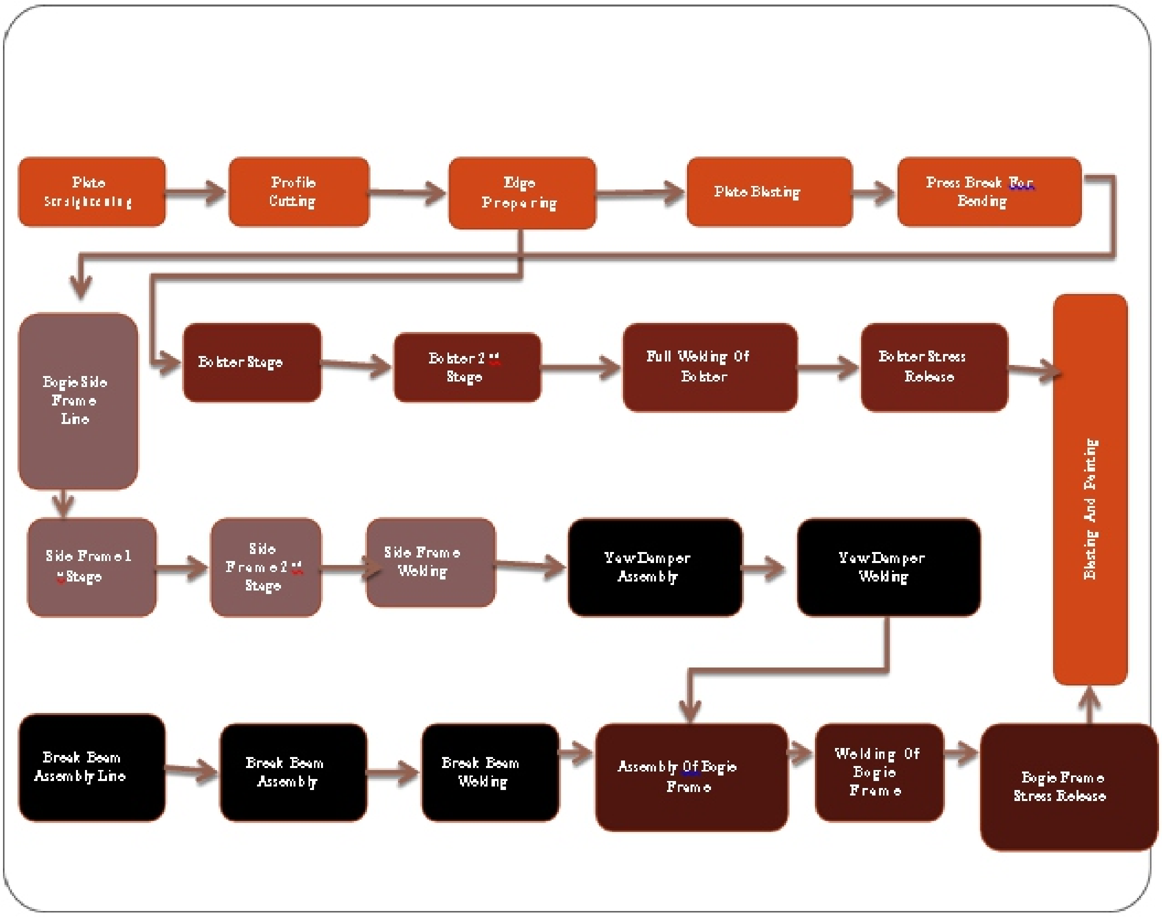

Fig.2 Flow process chart for manufacturing of bogies

4. RESEARCH METHODOLOGY

The Objective of this paper is to find the defects of the components and improve the manufacturing line using Quality control tools in assembly process so as to decrease the dismissals, and to upgrade client satisfaction.

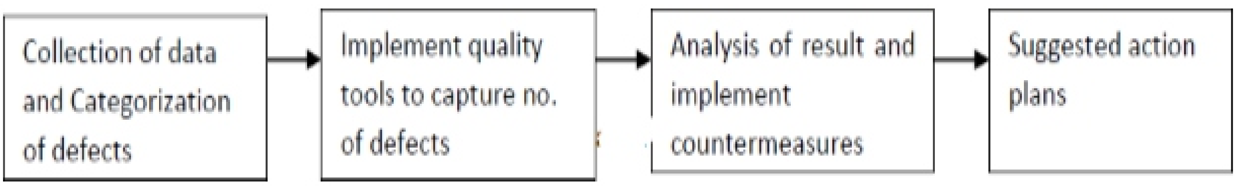

4.1 Data Collection

There are so many quality related issues which were seen at the work in industry. Rejection of materials because of imperfections has been observed in the assembly process of the manufacturing; as shown in Table1.

Table 1 List of parts of bogies produced in 2018-19

S. No.	Product Descriptions of bogie parts	Total quantity produced
1	Mating blocks	2738
2	Control arms	10882
3	Bolster guide	2850
4	Anker links blocks	5929
5	Guide of conventional bogie frame	1447
TOTAL		**23846**

Analysis of Defects

Various defects found during the operations are discussed in this sub-section.

4.2.1 Under size of Mating block

Mating block is part of the bogie bolster which is welded on its end. This defect will arise due to the human error. Due to this defect the machining cannot be done as the pointer of the machine cannot detect, from where the machining should be done.

As soon as, this defect is observed by the operators, it is to be rectified immediately. This can be removed by the filling of same material at the void (due to which the cutting machine was not able to find the start of cutting point). Fig. 3(a& b) shows the Mating block before and after machining.

(a)

(b)

Fig. 3 (a) Mating block before machining and (b) Mating block after machining 4.2.2Fault in Control Arm

The Figure 4 shows the control arms; which are welded on the side frame of the bogie. These are used for the fitting of the dampers. This defect occurs when machine did not cut the circumference with proper depth, as shown in Figure 4(b).

(a) (b)

Fig.4 (a) control arm before cutting by machine and(b) control arm with improper depth of cutting

If this is not rectified according to drawing then no further operations can be done due to dimensional error in the control arm circumference.

4.2.3 Gap between pair of control arms

There are 8 control arms used in the assembly of single bogie. They are always welded in pairs, so there are four pairs welded to the side frames of the bogie. Sometimes; during the welding the required gap between the control arm pairs may not according to the drawing. To rectify this defect; a rod will be welded between the pair of the control arms, so during the handling or doing other operations the gap between the pairs will remains same but when this assembly will go to the wheel assembly this rod is required to be cut, as shown in Figure 5 (a & b).

(a) (b)

Fig.5 (a) Gap between control arms and (b) Gap between control arms after rectification

4.2.4 Unequal levelling of Bolster's guide holes

This defect occurs in the bolster guide hole and this guide hole is used to assemble the bolster with the bogie frame. Figure 6 (a & b) shows the bolster guide holes of both types.

(a) (b)

Fig.6 (a)Improper level of bolster guide hole and (b) rectified guide hole after machining and boring

This error can be rectified by heating the unlevelled surface, and now machining can be done properly. There are 4 guide holes on the bolster

4.2.5 Ankerlink Blocks

The Ankerlink blocks are welded on the cross beams. These are welded in pair. There are 2 pairs of Ankerlink block in one bogie. These blocks are used to support the traction centre which is used for the fitting of bolster pin which will come through traction centre. This defect occurs due to improper welding but this defect may be rectified by heating. Fig.7 shows the Ankerlink blocks with improper gap and animated view of the setup.

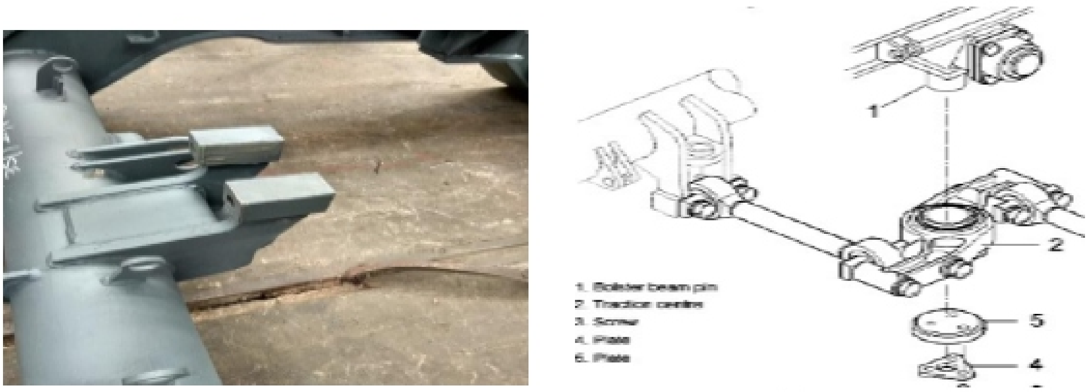

(a) (b)

Fig. 7 (a) Ankerlink blocks with improper gap and (b) Animated view of the setup

4.2.6 Distortion in guide of bogie frame

The guide of the bogie is used to bring bogie to a lower position. Sometimes, there is a distortion in this guide, as it gets tilted in one direction due to the improper welding. This defect can reduce the life of the bogies. Fig.8 shows the distortion in guide of bogie frames.

Fig. 8 Distortion in guide of bogie frames

5. APPLICATION OF QUALITY CONTROL TOOLS:

In this paper two quality tools namely; Pareto Chart and Cause & Effect diagrams are used to find the numbers and percentages of causes of defects and their possible rectification to improve the quality of the products/ assembly of the Railways.

5.1 Pareto chart

The Pareto principle, suggested by Italian economist; Vilfredo Pareto (also known as the 80/20 rule, the law of the vital few, or the principle of factor sparsity) states that, for many events, roughly 80% of the effects come from 20% of the causes. Pareto chart is a kind of diagram where the plotted qualities are arranged from biggest to smallest. A Pareto chart is used to feature the most regularly happening imperfections, the most widely recognized reasons for deformities, or the most of the causes. Various types of defects in the manufacturing of various parts of bogies are categorized in Table 2 and their graphical representation is shown in Figure 2.

Table 2 Types of defects in the manufacturing of various parts of bogies

S. No.	Name of Defect	No. of Rejections	Percentage of Rejections	Cumulative Rejection	Cumulative Rejection in %age
1	Fault in Control Arm	1829	35.32	1829	**35.32**
2	Ankerlink Blocks	1520	29.35	3349	**64.67**
3	Gap between pair of control arm	980	18.92	4329	**83.59**
4	Unequal levelling of Bolster's Guide hole	331	6.39	4660	**89.98**
5	Undersize of Mating Block	323	6.23	4983	**96.22**
6	Distortion in Guide of Bogie Frame	196	3.78	5179	**100**

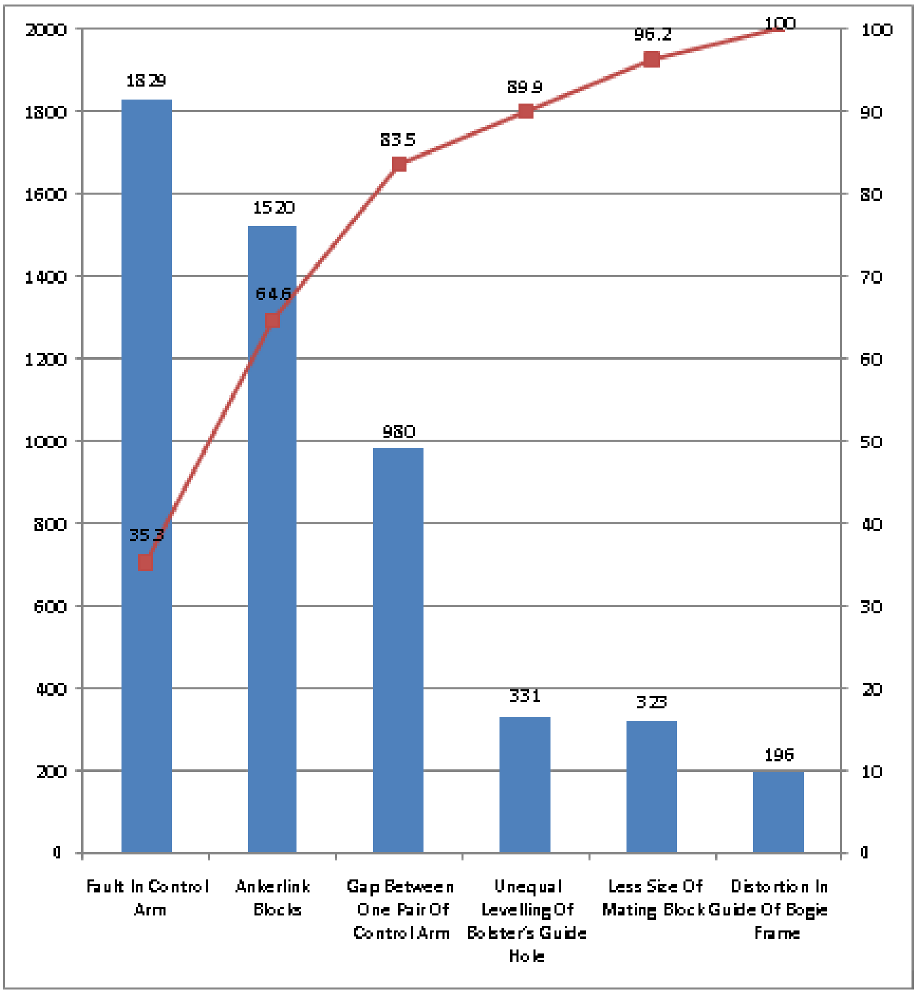

Fig.9 Pareto chart for analysis of defects in manufacturing in bogie shop

It is found from the Pareto chart that fault in control arms accounted for 35.3%, while is Ankerlink block accounts for 29.35%. Similarly, defects due to gap between pair of control arms are approximately 19%. These are the main defects which are responsible for about 84% of defects. So for these defects, Cause and Effect diagrams for each one are shown in the following sub-section.

5.2 Cause and Effect or Fishbone diagram(Ishikawa diagram)

Cause and Effect diagram are frequently arranged into four major's categories. These categories can be anything: Manpower, Methods, Materials and Machinery. Figure 10 shows the Cause and effect diagram for fault in control arm connection.

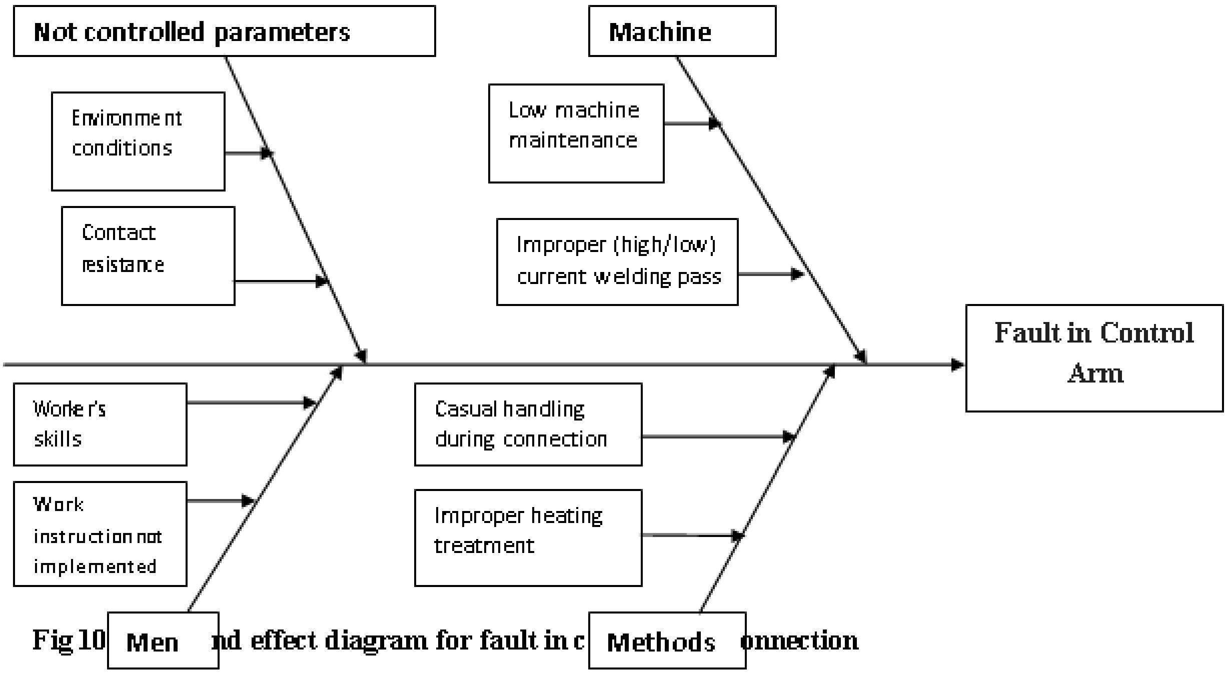

Fig 10 nd effect diagram for fault in c onnection

Figure 11 shows the Cause and effect diagram for fault in deflection of Ankerlink blocks.

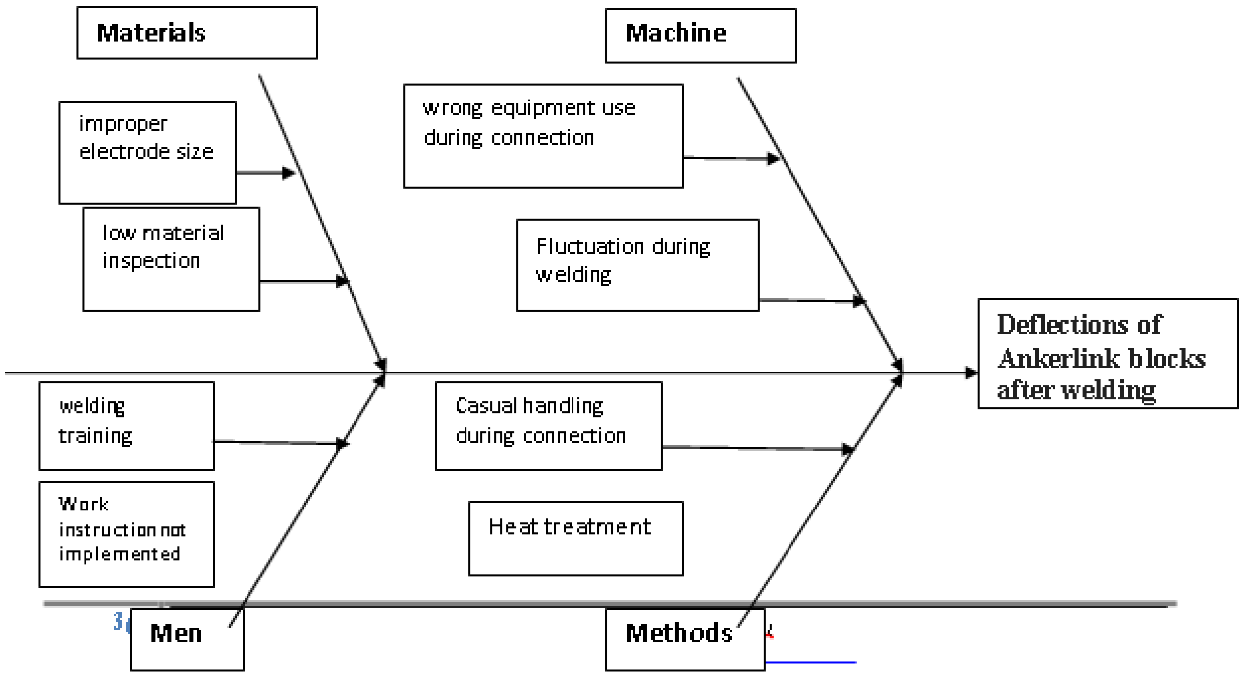

Fig.11 Cause and effect diagram for fault in deflection of Ankerlink blocks

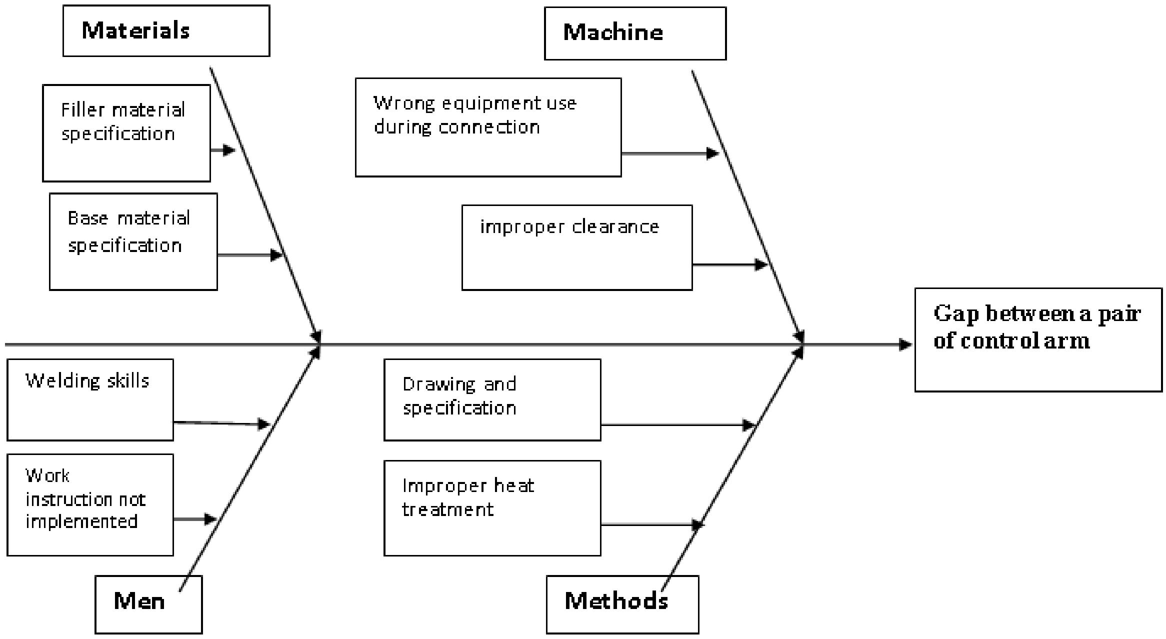

Fig 12 Cause and effect diagram for gap between a pair of control arms

5.3 Suggested action plans

Tables 3, 4 and 5 present the corrective action plans to improve the quality of products.

Tables 3 Action Plan for faults in Control arm

Category	Suggested actions
MACHINE	(i) To give the maintenance to the machine time to time, so it will give no fluctuation.
	(ii) Set appropriate current of welding machine according to the requirement.
MEN	(i) To give the required training to the worker.
	(ii) To give every machine instruction to the worker to avoid the deformities.
METHOD	(i) Do not do any casual handling during the connection.
	(ii) To give right amount of heat during treatment.

Tables 4 Action plan for deflection in Ankerlink blocks

Category	Suggested actions
MATERIAL	(i) Must use right kind of electrode to welding.
	(ii) Must do the inspection of the material.
MACHINE	(i) Use right equipment during welding.
	(ii)Set appropriate current of welding machine according to the requirement.
MEN	(i) Give right welding training to the worker.
	(ii) Give every machine instruction to the worker to avoid the deformities.
METHOD	(i) Avoid casual handling
	(ii) Appropriate heat treatment after welding

Tables 5 Action plan for gap between a pair of control arms

Type	Suggested actions
MATERIAL	(i) Study the specification of filler material
	(ii) Study the specification of base material
MACHINE	(i) Use right equipment during connection
	(ii) Use proper clearance during operation
MEN	(i) Give every machine instruction to the worker to avoid the deformities.
	(ii) Give proper training to the semi skill workers
METHOD	(i) Give proper heat treatment
	(ii) Read properly the drawing.

6. CONCLUSIONS

Quality prompts improvement in efficiency and it likewise upgrade the consumer loyalty and satisfaction. Study has been directed to execute quality control tools and procedures in manufacturing and assembling industry of Indian railways. The principle objective of this research paper is distinguish the deformity and propose a superior reason for improve the manufacturing line by implementing the Quality control tools in manufacturing and assembly process of railways bogies so as to reduce the non conformities. Quality control tools like Pareto chart and Cause and effect diagram have been used to distinguish various imperfections and reasons for these non conformities. Quality Control Tools can improve process execution by diminishing item variability and improves production effectiveness by decreasing scrap and framework.

REFERENCE

1. *Chen, M.S., Wu, M.H. and Lin, C.M.,(2014), "Application of indices Cp and Cpk to improve quality control capability in clinical biochemistry laboratories", The Chinese journal of physiology, vol. 57(2), pp. 63-68*
2. *Chan, C.L., Tse, A.C. and Yim, H.K., (2003), "Comparing and combining individual - charts and x-bar charts", International Journal of Quality & Reliability Management, Vol. 20 Issue: 7, pp.827 – 835.*
3. *Costa, A.F.B.(1999): "Joint X and R charts with variable sample sizes and sampling intervals", Journal of Quality Technology, Vol. 31, No. 4, pp. 387 – 397.*
4. *Das, N. and Sachan, L., (2013), "Robust control charts for controlling location parameter", International journal of Productivity and Quality Management, Vol. 12, No.1, pp.18 – 37.*
5. *Gaafar, L.K. and Keats, J.B.,(1984), "Statistical Process Control: A Guide for Implementation", International Journal of Quality & Reliability Management, Vol. 9 Issue: 4, pp. 9–20*
6. *Kemenade, E.V. and Hardjono, T.W.,(2018), "Twenty-first century Total Quality Management: the Emergence Paradigm", The TQM Journal, Vol.42, No.1, pp.77-89.*
7. *Prajapati, D.R. and Mahapatra, P.B., (2007), "An effective joint X-bar and R chart to monitor the process mean and variance", International journal of Productivity and Quality Management, Vol.2, No.4, pp.459 – 474.*
8. *Prajapati, D.R. and Singh, S., (2014), "Effect of warning limits on the performance of the X chart under autocorrelation", International journal of Productivity and Quality Management, Vol.13, No.2, pp.235 – 250.*
9. *Ronald, D. and Fricker, J.,(2009), "Optimising Shewhart charts in parallel production lines", International journal of quality engineering and productivity, Volume 1 No. 2 pages 125- 135.*
10. *Saniga, E., McWilliams, T., Davis, D. and Lucas, J., (2006), "Economic control chart policies for monitoring variables", International journal of Productivity and Quality Management, Vol.1, No.1/2, pp.116 – 138.*
11. *Singh, A., and Prajapati, D.R., (2016), "Implementation of SPC tools for process Improvement: A Case Study", International Journal of Management, IT & Engineering, Vol. 6 Issue 9, pp.223-237.*

An Effective Method for Fire Analysis of Steel Frames

[1] Viet-Linh Tran, [2] Viet-Hung Truong, [3] Thai-Hoan Pham, [4] Duc-Kien Thai, [5] Seung-Eock Kim

[1,2]PhD Student, Dept. of Civil and Environmental Engineering, Sejong University.
[2]PhD, Dept. of Civil Engineering, Vinh University, 182 Le Duan, Vinh City, Viet Nam
[3,4]Professor, Dept. of Civil and Environmental Engineering, Sejong University, 98 Gunja-dong, Gwangjin-gu, Seoul, 143-747, South Korea
E-mail: [1]vietlinhdhv@sju.ac.kr, [2]truongviethung82@sju.ac.kr, [3]Pth.thebasic@gmail.com, [4]thaiduckien@sejong.ac.kr, [5]sekim@sejong.ac.kr

A B S T R A C T

This paper presents a developed method using practical advanced analysis (PAA) for fire analysis of steel frames. PAA based on the beam-column approach is employed to obtain the nonlinear inelastic behaviors of structure. The fire effects on structural behavior of steel frames are estimated by taking into account the degradations of elastic modulus, yielding strength, and thermal force at elevated temperature. The calculated results are then compared with the test results to demonstrate the accuracy of the proposed method.

Keywords- Fire Analysis, Practical Advanced Analysis, Steel Frame.

I. INTRODUCTION

PAA methods allow the direct capture of nonlinear inelastic behaviors of steel structures. Liew et al. [1] and Iu and Chan [2] have used this method for fire analysis of structures. However, the results from these studies might not reliably reflect the behavior of structures under fire effects since $P-\delta$ effect has not been considered. Besides, Chen and Hwa [3] have used advanced analysis to determine the survival time of steel frames under elevated temperature. Nevertheless, this approach was limited in two-dimensional formulation case.

To address the aforesaid limitations, we propose an efficient method for fire analysis of steel frames used in three-dimensional formulation. In order to demonstrate the accuracy of the proposed method, the analysis results are compared with tests.

II. PRACTICAL ADVANCED ANALYSIS

The beam-column approach used for practical advanced analysis was presented in the work of Kim et al. [4]. Accordingly, the $P-\delta$ and $P-\Delta$ effects are accounted by using stability functions, while the CRC tangent modulus concept is used to account for residual stresses and initial geometric imperfection. A parabolic function model is used to represent the transition from elastic to zero stiffness associated with a developing hinge. This formulation was successfully used for analyzing the steel frames subjected to the static load.

III. PRACTICAL ADVANCED ANALYSIS IN FIRE

The degradation of the yield strength and elastic modulus of steel material at the elevated temperature leads to a decrease of structural stiffness. Those degradations are determined using the mathematical models proposed by Chen and Hwa [3]. In this analysis, the internal forces caused by thermal expansion are also treated as equivalent forces due to temperature change. The fire analysis of steel structures is presented in the following sub-sections.

A. The Internal Forces Due To Temperature Effects

According to Kim et al. [4], the incremental force-displacement relationship of beam-column element is written as:

$$\{\Delta F\} = \left[K_{ij}\right]\{\Delta D\}, \qquad (1)$$

where $\{\Delta F\}$ and $\{\Delta D\}$ are the incremental force and displacement vectors, respectively; and $[K_{ij}]$ tangent stiffness matrix.

Assuming that the temperature through cross section is uniform, Eq. (1) considering the effect of temperature can be expressed as:

$$\{\Delta F\} = \left[K^T_{ij}\right]\{\Delta D\} - \{\Delta F_T\}, \qquad (2)$$

where T is the elevated temperature; $\left[K^T_{ij}\right]$ is the tangent stiffness matrix at T; and $\{\Delta F_T\}$ is the incremental thermal load vector, which is written as:

$$\{\Delta F_T\} = \{E_T A \alpha \Delta T \quad 0 \quad 0 \quad 0 \quad 0 \quad 0\}^T, \qquad (3)$$

in which $E_T A$, α, ΔT are the axial stiffness, coefficient thermal expansion, and incremental temperature, respectively. In this study, α is assumed to be equal to $14 \times 10^{-6} C^{-1}$.

B. Fire analysis of steel frames

In the proposed procedure, the structural static analysis under applied loads is firstly performed, and fire analysis is then carried out. In fire analysis, the unbalanced forces of the structure due to temperature change are calculated based on the difference between the internal and external forces. The incremental displacements of the structure corresponding to these unbalanced forces are computed and then added to the total displacement of the structure. This process is repeated until the equilibrium between internal and external forces is satisfied. So on, a new thermal increment can be imposed to the structure to restart the procedure.

IV. VERIFICATION

To illustrate the accuracy of the proposed method, two different examples are calculated and verified.

A. Simply supported beam

A simply supported beam with uniformly heated along the entire length as shown in Fig. 1, tested by Rubert and Schaumann [5], is used for the first verification. The section of the beam is IPE80. At ambient temperature, the elastic modulus (E_{20}) is equal to $210x10^3$ N/mm^2, while the yield strengths (fy_{20}) are equal to 401 N/mm^2 and 399 N/mm^2 corresponding to the ratio F/F_u (the applied/ultimate load) = 0.2 and 0.5, respectively.

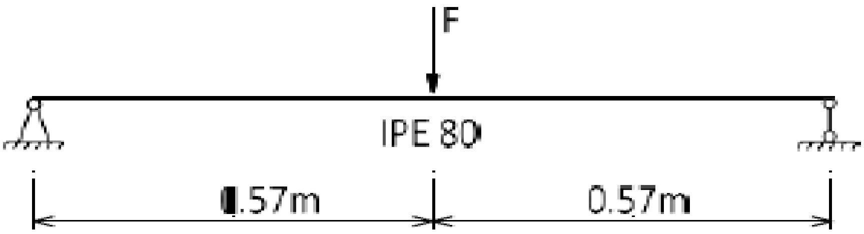

Fig. 1. Simply supported beam

Fig. 2 compares the displacement – temperature relationship at mid-span between the proposed method and the test results. It can be seen that the present results shows a good agreement comparing with the test results.

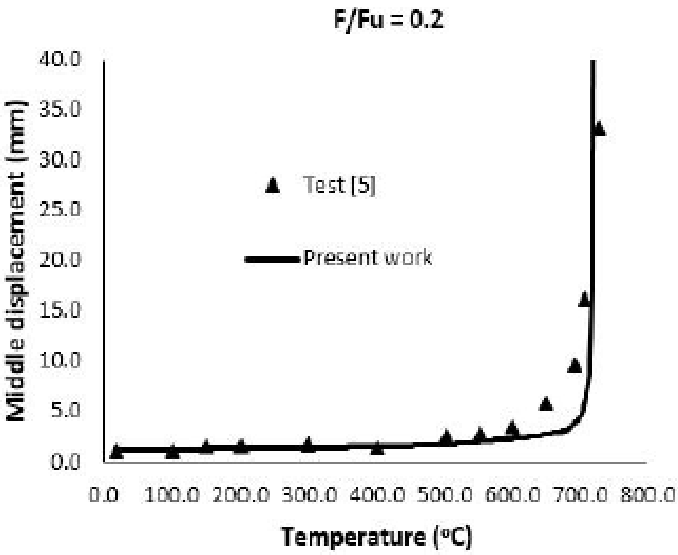

(a)

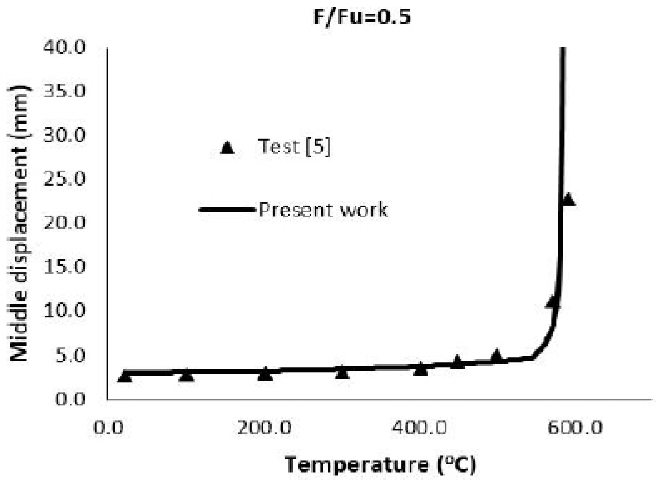

(b)

Fig. 2. Temperature-displacement relationship at mid-span of the simply supported beam

B. Inverted L-shaped frame

Another test of Rubert and Schaumann [5] on the inverted L-shaped frame, as shown in Fig. 3, is used for the second verification. In this case, E20 is equal to 210x103 N/mm2 and fy20 is equal to 382 N/mm2 at ambient temperature.

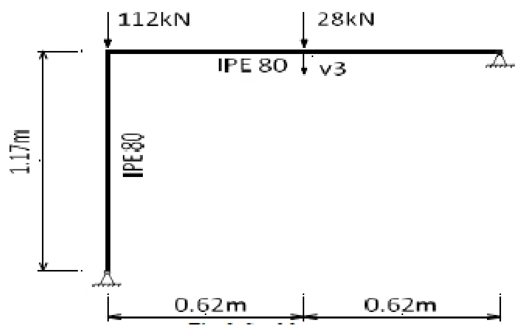

Fig. 3. Steel frame

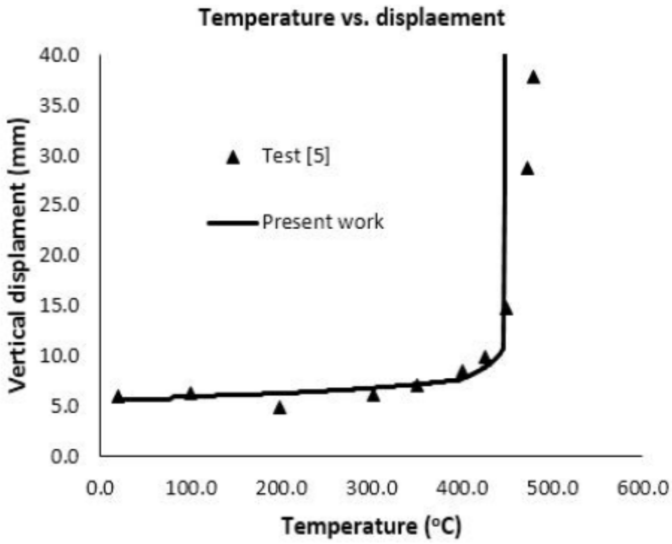

Fig. 4. Temperature –vertical displacement (v3) relationship

Fig. 4 shows the relationship between the vertical deflection (v3) and temperature. It illustrates a reasonable agreement between the present work and the given test.

CONCLUSION

The Following Conclusions Are Drawn From This Study:

1. An effective method using practical advanced analysis with three-dimensional formulation is proposed for fire analysis of steel frames.
2. The good comparisons between the present work and the test results demonstrate that the proposed procedure is accurate.

REFERENCES

[1] J.Y. Liew, L.K. Tang, T. Holmass, and Y.S. Choo, "Advanced analysis for the assessment of steel frames in fire," Journal of Constructional Steel Research, vol. 47, pp. 19–45, 1998.

[2] C.K. Iu and S.L. Chan, "A simulation-based large deflection and inelastic analysis of steel frames under fire," Journal of Constructional Steel Research, vol. 60, pp. 1495-1524, 2004.

[3] W.F. Chen and K. Hwa, "Survival Time Prediction of Steel Frame under Elevated Temprature Using Advanced Analysis," Steel Structures, vol. 4, pp. 187-196, 2004.

[4] S.E. Kim, M.H. Park, and S.H. Choi, "Direct design of three dimensional frames using practical advanced analysis," Engineering Structures, vol. 23, pp. 1491-1502, 2001.

[5] A. Rubert and P. Schaumann, "Structure steel and plane frame assemblies under fire actions," Fire Safety Journal, vol. 10, pp. 173-184, 1986.

Performance Evaluation of Shear-Wall on Existing Irregular Building under Seismic Loadings

[1] Subhrajit Das, [2] Supradip Saha
[1]B.Tech 4th year student,
[2]Assistant Professor,
[1,2]Department of Civil Engineering (FST), The ICFAI University Tripura, India-799210 Email:
[1]dasjit44@gmail.com, [2]supradipsaha@iutripura.edu.in

ABSTRACT

The present paper deals with the performance evaluation of shear-wall in reducing the structural response of existing irregular building subjected to earthquake loadings. For evaluating the effectiveness of shear wall, seismic analysis was conducted on the structure with and without shear-wall. Seismic analysis like Linear Static Analysis, Response Spectrum Analysis and Time History Analysis has been performed in STAAD Pro V8i to obtain the response of the building under various loading. Effect of static load and live load along with dynamic response under the above mentioned analysis methods have been meticulously analyzed. After analyzing the results, it was observed that dynamic analysis of any irregular structure of height more than 12 m, located at vulnerable seismic zones like zone IV and V is very essential for safe design consideration since the same with static analysis does not produce the critical design parameters. It has also been observed that implementation of shear wall on the structure is more significant and effective to reduce its seismic response.

Keywords - Structural Response, Linear Static Analysis, Response Spectrum, Time History, Shear-wall.

I. INTRODUCTION

The present trend of constructing multi storey buildings or sky scrapers is mainly due to the fact that people don't get much space to expand horizontally. This makes the multi storey structures vulnerable to the seismic effects as they become comparatively light in weight, flexible and moderately damped. When lateral loads act on these structures, they undergo vital vibration which is not acceptable against the safety and serviceability of the structure. The branch of structural dynamics witnessed numerous research works on seismic analysis over virtual models that were non-existing structures, where things are often regular, ideal and limited to various assumptions regarding the modelling. The case may not be the same for existing structures where they are irregular in shape or consist of expansion joints or might be with a complicated architecture. So for the safety of such structures, structural engineers are in operation to work out different kinds of structural systems that can mitigate the damaging effects of seismicity. These systems work by absorbing or reflecting a portion of the input energy that might rather be transmitted to the structure itself. One of the structural response mitigation techniques is the application of shear-wall in the structure. In this present paper, the focus is primarily on the performance evaluation of shear-wall on the academic building of the ICFAI University, Tripura by performing seismic analysis on it and also to study the effectiveness of shear-wall in reducing the structural response of the existing building. Linear Static Analysis, Response Spectrum Analysis and Time History Analysis have been performed to study the response of the building under various loading. Effect of static load and live load along with dynamic response under linear static, response spectrum and Time History has been meticulously analysed. The various parameters that are considered for conducting the comparative study are storey shear, storey drift and average displacement for linear static analysis, average displacement for response spectrum and storey drift and average displacement for time history. The comparative response of the building due to static loading and dynamic response spectrum has also been explored to sense the importance of dynamic analysis over static analysis by monitoring the parameters like shear force, bending moment, axial load and displacement.

Several research works regarding this context were made in the past, such as Sardar and Karadi (2013) investigated the effect of change in shear wall location on storey drift of multi storey building subjected to lateral loads. NazmulHaq et al. (2013) evaluated the dynamic behaviour of the structure by performing dynamic analysis of a 15 storey R.C.C building with varying height. Ravikanth and Ramancharla (2014) conducted a study on significance of shear wall in high-rise irregular buildings as it can be very efficient in resisting lateral loads originating from wind or earthquakes. Kumar et al. (2014) studied the performance of shear walls in R.C. structures. Gupta and Pande (2014) studied the effect of placement and openings in shear wall on the displacement at various levels in a building subjected to earthquake loads. LovaRaju and Balaji (2015) conducted non-linear pushover analysis on four types of frames and the frames were compared with pushover curves. Kabir et al. (2015) investigated the seismic vulnerability and Response of multi-storey regular and irregular buildings of identical weight under static and dynamic loading in context of Bangladesh. Ramchandani and Mangulkar (2016) compared different shapes of structure by performing Response Spectrum Analysis. Chouhan and Makode (2016) performed dynamic Analysis of Multi-Storey Frame-Shear Wall Building Considering Soil Structure Interaction.

The objective of this present study is to assess the effectiveness of shear-wall on the academic building of the ICFAI University, Tripura by performing seismic analysis in various methods and also to determine the effectiveness of implementing shear- wall for reducing structural response.

II. DETAILS OF BUILDING AND STRUCTURAL MODELING

The Academic building of The ICFAI University, Tripura is a 5-Storey irregular building having each floor height of 3.6m and spanning over a length of 120m and 46m in both X and Y direction respectively (as shown in Fig. 1). The dimensions of the columns are 300mm × 600mm and beams are of 300mm × 400mm. The shear-wall introduced for the study was at the corner sides of the building for mitigating the response (as shown in Fig. 2).

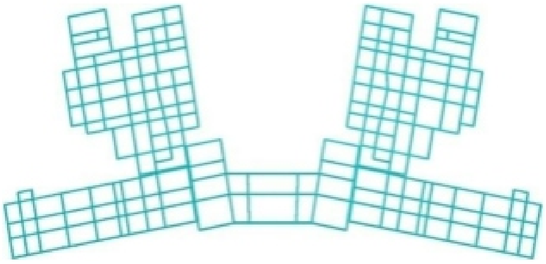

Fig.1. Plan of the Academic building of the ICFAI University, Tripura modeled in STAAD Pro V8i

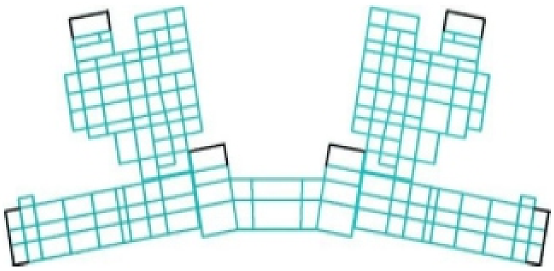

Fig.2. Plan of the Academic building of the ICFAI University, Tripura with shear-wall at the extreme corners and sides modeled in STAAD Pro V8i

III. METHODOLOGY

The purpose of dynamic analysis is to obtain the design seismic forces, with its distribution to different levels along the height of the building and to the various lateral load resisting elements similar to equivalent lateral force method. For the analysis it is assumed that masses are lumped at the storey level and only sway displacement is permitted in each storey. The design lateral force acting at each floor is determined by the following formula,

$$Q = A_h P_k \phi_{ik} W_i$$

where,

A_h – horizontal acceleration coefficient

P_k – participation factor of each mode

ϕ_{ik} – mode shape coefficient

W_i – seismic weights of each floor

Since for the present study the software STAAD Pro V8i is used for analysis, thus as inputs the particulars that needs to be provided to prepare a seismic definition for enabling the software to carry out the Response Spectrum Analysis are as follows.

- Zone factor (Z) = 0.36
- Damping Ratio = 0.05
- Importance factor (I) = 1.5
- Response reduction factor (R) = 5
- Time period (Ta) in sec $= \dfrac{0.09 \times h}{\sqrt{d}} = 0.148,\ 0.239$ (for X and Y direction respectively)
- Lumped weight = 12 KN/m & 10 KN/m for ground to 3rd floor and roof respectively
- Live load = 6 KN/m2 & 1.5 KN/m2 for ground to 3rd floor and roof respectively
- Modal combination method = SRSS (Square root of Sum of Squares)
- Soil class = Medium soil
- Multiplication factor of average response acceleration coefficient $\left(\dfrac{Z}{2} \times \dfrac{I}{R}\right) = 0.0054$
- Shear wall thickness = 300 mm

IV. RESULTS AND DISCUSSION

Investigations are conducted to study the behavior of a structure by performing different types of seismic analysis with and without shear wall. In this study, shear drift, storey shear, displacement of the structure with and without shear wall are measured. The results obtained in this experimental study have been plotted hereafter.

4.1. Linear Static Analysis

This is a static analysis in which the design base shear is calculated and hence the peak storey shear as well as the lateral loads acting on each floor is determined. These lateral loads act as horizontal point loads on the structure during the analysis.

4.1.1 Variation of storey shear with and without shear-wall

The variation of storey shear of the building with and without shear-wall has been analyzed and shown in Table 1 and Fig. 3. It was observed that the maximum storey shear of the structure with and without shear- wall was 946.318 KN and 1080.413 KN respectively.

Table 1. Comparison of storey shear with and without shear wall

Floor levels	Floor height (m)	Storey shear without shear wall (KN)	Storey shear with shear wall (KN)
5	18	187.805	166.434
4	14.4	210.328	200.043
3	10.2	594.447	571.707
2	7.2	897.041	843.59
1	3.6	1080.413	946.318
0	0	1080.413	946.318

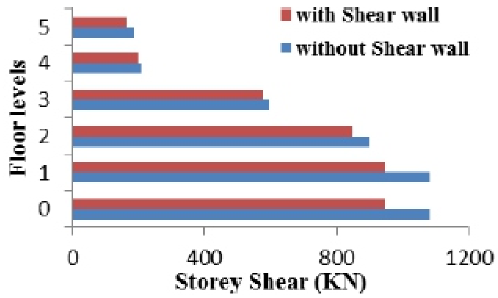

Fig. 3. Variation of storey shear in context to different floor levels with and without shear wall

4.1.2 Variation of storey drift with and without shear-wall

The variation of storey drift of the building with and without shear-wall has been analyzed to be 3.6 cm and 9.9 cm respectively as shown in Table 2 and Fig. 4.

Table 2. Comparisons of storey drift with and without shear wall

Floor levels	Floor height (m)	Storey drift without shear wall (cm)	Storey drift with shear wall (cm)
5	18	9.9739	3.6739
4	14.4	9.6538	3.3068
3	10.2	8.4029	2.583
2	7.2	6.2977	1.6263
1	3.6	4.5167	0.6216
0	0	0	0

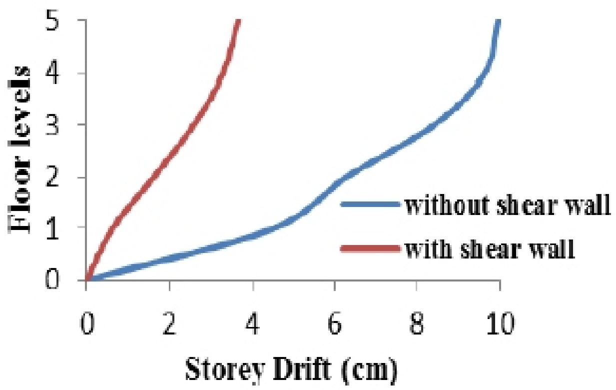

Fig. 4. Variation of storey drift in context to different floor levels with and without shear wall

4.1.3 Variation of displacement with and without shear-wall

The variation of displacement of the building with and without shear-wall has been analyzed. It is observed that the maximum displacement of the structure with and without shear wall was 8.6 cm and 24 cm respectively as shown in Table 3 and Fig. 5.

Table 3. Comparison of average displacement with and without shear wall from linear static analysis

Floor levels	Floor height (m)	Average displacement without shear wall (cm)	Average displacement with shear wall (cm)
5	18	24.0218	8.6852
4	14.4	21.3761	7.3521
3	10.2	16.7221	5.4891
2	7.2	10.8143	3.3153
1	3.6	4.5167	1.2253
0	0	0	0

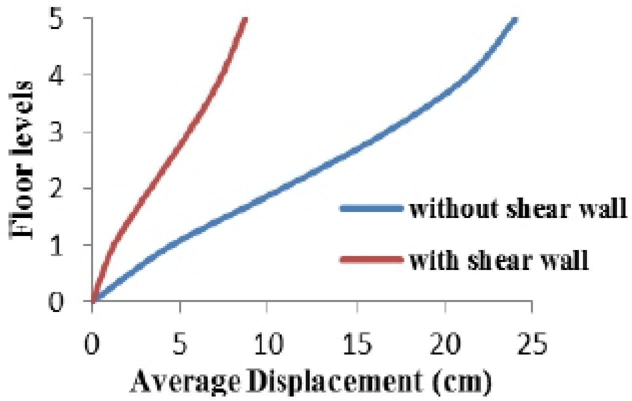

Fig.5. Variation of average displacement in context to different floor levels with and without shear wall

4.2 Response Spectrum Analysis

In this analysis depending on the soil type, the normalized spectral acceleration is set as the seismic load case, which is then used to analyse the structure. The analysis involves determining the maximum average displacement of the structure with and without shear-wall.

4.2.1 Variation of displacement with and without shear-wall

The variation of displacement of the building with and without shear-wall has been analyzed to be 43.6cm and 62.6cm respectively as shown in Table 4 and Fig. 6.

4.3 Comparison of seismic response of the structure on the basis of seismic analysis:

The present study reviews the seismic response of the academic building of the ICFAI University by performing the linear static analysis as well as the response spectrum analysis and compares both the analysis results. The parameters that we considered for the comparison are the maximum values of shear force, bending moment, axial force and displacement as shown in Table 5.

Table 4. Comparison of displacement with and without shear wall from response spectrum

Floor levels	Floor height (m)	Average Displacement without shear wall (cm)	Average Displacement with shear wall (cm)
5	18	62.6195	43.6304
4	14.4	56.8587	38.674
3	10.2	46.1064	30.4756
2	7.2	31.3798	19.5209
1	3.6	13.4991	7.5371
0	0	0	0

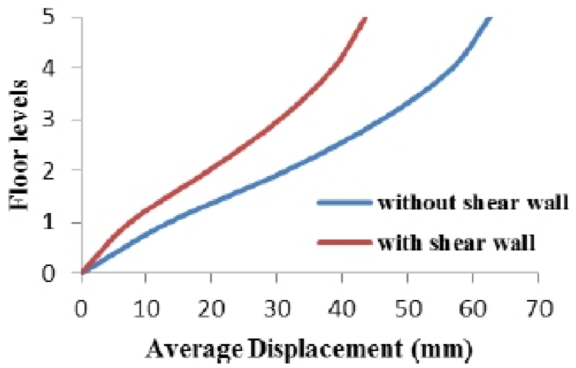

Fig.6. Variation of average displacement in context to different floor levels with and without shear wall

Table 5. Comparison of seismic response of the structure by linear static analysis and response spectrum analysis

Parameters	Linear Static Analysis	Response Spectrum Analysis	Percentile variations (%)
Shear Force (in KN)	18	62.6195	53.33
Bending Moment (in KN-m)	14.4	56.8587	28.12
Axial force (in KN)	10.2	46.1064	3.05
Displacement (in mm)	7.2	31.3798	29.97

After observing the above variations of the parameters, it is well clear that the results of response spectrum analysis are much critical than that of linear static analysis. Thus it is necessary to perform dynamic analysis of any irregular structure of height more than 12 m, located at vulnerable seismic zones like zone IV and V.

4.4 Time History Analysis

are illustrated below. From the analysis the time history that results in the maximum displacement of the structure is reanalysed with shear wall to characterize any improvement in the structural response.

4.4.1 The Coalinga Earthquake

After performing the analysis, the maximum displacement of the node 1421 was observed to be 106 mm, as shown in Fig. 7.

4.4.2 The Kobe Earthquake

After performing the analysis, the maximum displacement of the node 1421 was observed to be 112 mm, as shown in Fig. 8.

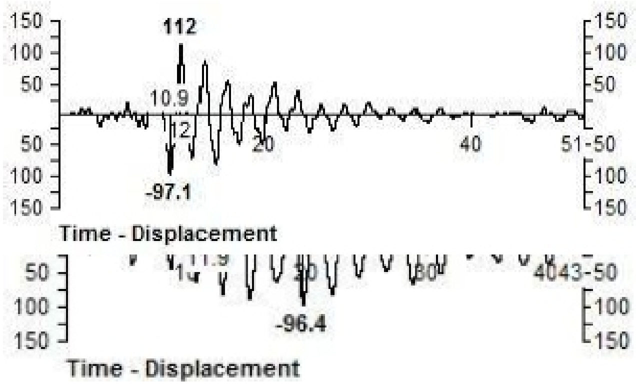

Fig. 8. Variation of Displacement with respect to time for node 1421 from the Kobe earthquake time history

4.4.3 The Mammoth Lake Earthquake

After performing the analysis, the maximum displacement of the node 1421 was observed to be 116 mm, as shown in Fig. 9.

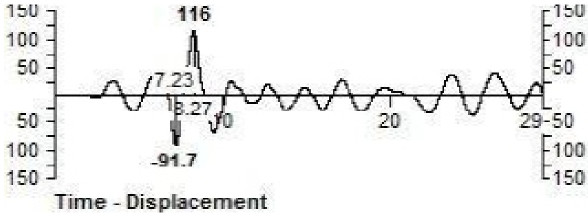

Fig. 9. Variation of Displacement with respect to time for node 1421 from the Mammoth Lake earthquake time history

The data of few time history accelerations of the seismic excitations occurred across the world were used to understand the behaviour of the structure in such real ground excitations. The observations reported that the beam-column joint numbered 1421 shows the maximum response and the time versus displacement graph for all the recorded time history

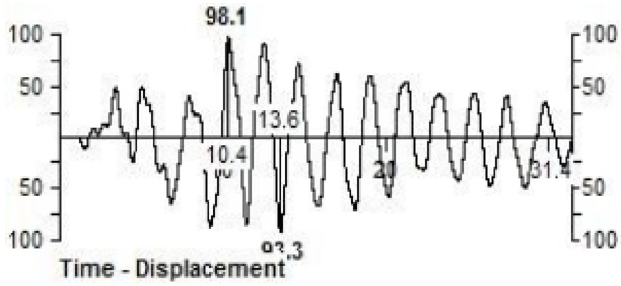

Fig. 10. Variation of Displacement with respect to time for node 1421 from the Imperial Valley earthquake time history

4.4.4 The Imperial Valley Earthquake

After performing the analysis, the maximum displacement of the node 1421 was found to be 98.1 mm, as shown in Fig. 10.

4.4.5 The Palm Spring Earthquake

After performing the analysis, the maximum displacement of the node 1421 was observed to be 91.2 mm, as shown in Fig. 11.

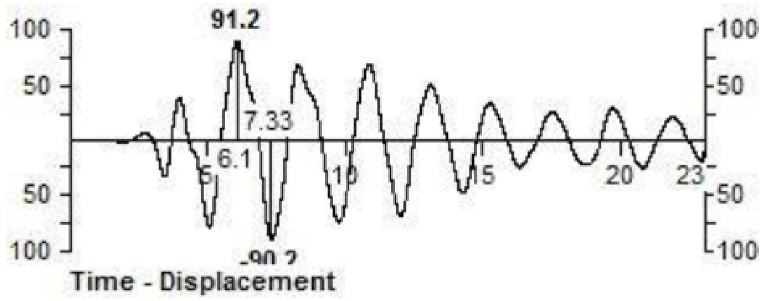

Fig. 11. Variation of Displacement with respect to time for node 1421 from the Palm Spring earthquake time history

After studying the above responses of various time history data(s), it can be inferred that the maximum displacement occurred in Mammoth Lake earthquake. Therefore, to study the effectiveness of shear wall in reducing the response, variation of displacement with time of the structure with shear wall has been illustrated below. It is found that, due to the implementation of the shear wall, value of maximum displacement of the beam column joint number 1421 is reduced to 71.7 mm as shown in Fig. 12.

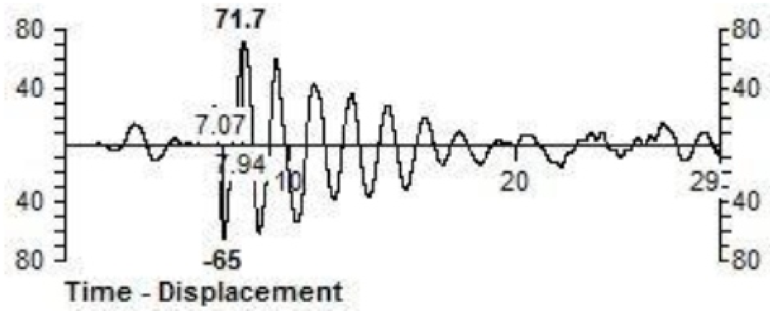

Fig. 12. Variation of Displacement with respect to time for node 1421 from the Mammoth Lake earthquake time history by implementing shear-wall on the structure

The variations over the parameters, like as average displacement and storey drift, with and without shear wall is also plotted in the Fig. 13 and 14 respectively. It can be easily observed that the implementation of shear wall effectively reduces the structural responses.

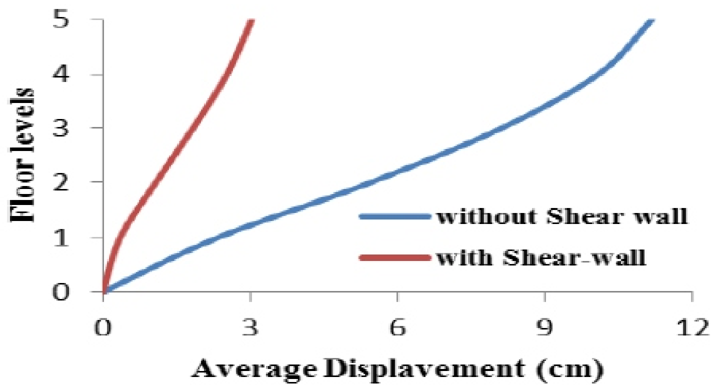

Fig.13. Variation of average displacement in context to different floor levels with and without shear wall for mammoth lake earthquake

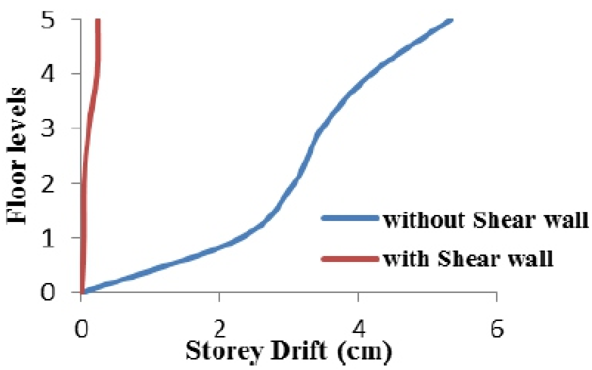

Fig. 14. Variation of storey drift in context to different floor levels with and without shear wall for mammoth lake earthquake

EFFECTIVENESS OF SHEAR-WALL

The effectiveness of shear-wall is calculated in terms of the reduction of the storey shear, storey drift and displacement parameters with shear-wall (Sw) and without shear-wall (So) as follows:

$$\psi = \left(\frac{S_o - S_w}{S_o} \times 100\right)\%$$

The comparative study of the response reduction by implementing shear-wall on the structure resulted in the reduction of storey shear, storey drift and displacement by 8.48%, 71.71% and 67.76% respectively in linear static analysis. The same was observed by response spectrum analysis, where the displacement was reduced by 35.63% meanwhile, in case of time history analysis the parameters like storey drift and displacement was reduced by 96.76% and 78.09% respectively.

CONCLUSIONS

The Linear static analysis has been performed over the academic building of the ICFAI University, Tripura with and without shear-wall, which reduced the seismic response of the structure in context to the parameters like storey shear, storey drift and average displacement by 8.48%, 71.71% and 67.76% respectively. The same was done by performing response spectrum and the average displacement of the structure was reduced by 35.63%. The response of the existing structure analysed by linear static analysis and response spectrum analysis considering the parameters like shear force, bending moment, axial force and displacement varied by 53.33%, 28.12%, 3.05% and 29.97% respectively. Since there is a considerable variation of the parameters taken above, it is well justified that irregular structures of height more than 12 metre in seismic zones IV and V shall be analysed by dynamic analysis for the safe design consideration. Lastly, behaviour of the existing structure was analysed by time history analysis where the structure gave maximum response in terms of maximum displacement of 116 mm from the Mammoth Lake earthquake. The response was reduced to 71.7 mm when the same structure was analysed using shear-wall. The shear wall proved to be effective enough by reducing the average displacement and storey drift of the structure during mammoth lake earthquake by 78.09% and 96.76% respectively. Therefore, it can be finally concluded that the implementation of shear wall effectively reduces the structural responses.

ACKNOWLEDGMENTS

Numerous works in the branch of structural dynamics has already been done by many resourceful authors. Yet, Prof. Supradip Saha guided me with the idea of performing this study on an existing structure over which comparatively less works were made, where the effect of seismology could be properly witnessed in a real sense. He also guided me to get all the insights of seismic analysis by providing necessary materials. Thus I take this opportunity to express my gratitude towards him and I look forward to work with him in the near future.

REFERENCES

[1] Sardar, S.J., Karadi, U.N., (2013), "Effect of change in shear wall location on storey drift of multistorey building subjected to lateral loads", IJIRSET Journal of Earthquake Technology, ISSN: 2319-8753, v. 2, issue 9, pp. 4241 - 4249.

[2] Haq, Md. N., And Chowdhury, Md. A., (2013), "Evaluation of the impact of dynamic analysis on different building height", International Journal of Science and Research (IJSR), India, ISSN: 2319-7064, v. 2, issue 8, pp. 204 – 207.

[3] Kumar, V.S., Babu, S., and Kranti, U., (2014), "Shear walls – A review", International Journal of Innovative Research in Science, Engineering and Technology, ISSN: 2319-8753, v. 3, issue 2, pp. 9691 – 9694.

[4] Gupta, P.R., and Pande, A.M., (2014), "Effect of placement and openings in shear wall on the displacement at various levels in a building subjected to earthquake loads", International Journal of Research in Engineering and Applied Sciences, ISSN (Online):2348-1862, v. 2, pp. 5–9.

[5] Ch, R., and Ramancharla, P.K., (2014), "Significance of shear wall in high-rise irregular buildings", International Journal of Education and Applied Research, ISSN: 2348- 0033 (Online), v. 4, issue 2, pp. 35 – 37.

[6] LovaRaju, K., and Balaji, Dr.K.V.G.D., (2015), "Effective location of shear wall on performance of building frame subjected to earthquake load", International Advanced Research Journal in Science, Engineering and Technology, ISSN: 2393-8021, v. 2, issue 1, pp. 33 – 36.

[7] Kabir, Md.R., Sen, D., and Islam. Md.M., (2015), "Response of multi-storey regular and irregular buildings of identical weight under static and dynamic loading in context of Bangladesh", International Journal of Civil and Structural Engineering, ISSN 0976 – 4399, v. 5, pp. 252 -260.

[8] Ramchandani, J.R., and Mangulkar, M.N., (2016), "Comparison between different shapes of structure by response spectrum method of dynamic analysis", Open Journal of Civil Engineering, v. 6, pp. 131-138.

[9] Chouhan, M., and Makode, R.K., (2016), "Dynamic analysis of multi-storeyed frame-shear wall building considering SSI", International Journal of Engineering Research and Application, ISSN: 2248-9622, v. 6, issue 8, pp. 31- 35.

ISSN. Application No. 21794

Influence of Blast Load Modelling on Dynamic Response of Structures

[1] **Michał Lidner,** [2] **Zbigniew Szczesniak**
Faculty of Civil Engineering and Geodesy, Military University of Technology, Poland
Email: michal.lidner@wat.edu.pl, zbigniew.szcześniak@wat.edu.pl

A B S T R A C T

The paper presents a new own method of modeling of the air shock wave generation and propagation. Conception of the method refers to the idea of Finite Volume Method and takes into account energy losses with respect to an adiabatic process rule. A charge explosion in the air was analyzed. A congeneric simulation was done considering spatial propagation of post-explosion gases and air shock wave and also dynamic response of isolated structural element.

Index Terms- Adiabatic Process Rule, Blast Load, Dynamic Response, Finite Volume Method

I. INTRODUCTION

When considering human activity nowadays one can meet the blast load over pressure caused by different actions. From the point of view of people and building security one of the main destroying factors is the air shock wave. Rational estimating of blast load results should be preceded with knowledge of complex wave field distribution in time and space. As a result one can estimate the blast load distribution in time and space applied to structural elements. In technical conditions, the values of blast load are estimating using the empirical functions of over pressure distribution in time ($\Delta p(t)$) [1]-[7]. The $\Delta p(t)$ functions are monotonic and are the approximation of reality.

Additionally, distributions of these functions are often linearized due to simplifying of estimating the blast reaction of elements.

The ability to estimate blast load overpressure properly plays an important role in safety design of covers, shelters and also buildings. This issue is much more important when the space affected by explosion is inhibited by several factors. In such situations scientific papers consider often simplified conception of blast load and its reflection. When considering mentioned references authors think that the more development of air shock wave propagation and blast load distribution in time is needed.

II. GENERAL CHARACTERISTIC OF BLAST LOAD MODELING

A. Shock Wave Region

The unknown Δp(t) function reflects the thermodynamic state in each point of disturbed gaseous medium, and also reflects the influence of the boundary conditions. The most advanced models available nowadays for Computational Fluid Dynamics are based on Finite Volume formulations, expressing the conservation of mass, momentum and energy) are formulated and solved in conservative form (see ref. [8]). Thus conservation of mass, momentum and energy in gaseous medium about the density equal to ρ can be written as follows:

$$\frac{\partial}{\partial t}\iiint_V \rho dV + \iint_S \rho v_n dS = 0, \qquad (1)$$

$$\frac{d}{dt}\left(\iiint_V \rho \vec{v}\, dV\right) = \iint_S p_n dS + \iiint_V \rho \vec{F}_m dV, \qquad (2)$$

$$\frac{d}{dt}\left[\iiint_V \rho\left(c_v T + \frac{v^2}{2}\right) dV\right] = \iint_S p_n v_n dS + \iiint_V \rho \vec{F}_m \vec{v}\, dV + \qquad (3)$$

$$+ \iint_S \dot{q}_n dS + \iiint_V \dot{q}_m \rho dV,$$

in which the governing equations for the fluid domain (equations for a compressible inviscid fluid, where: t – time, S – surface area of the considered finite volume about volume equal to V, v_n – flow rate of the gaseous medium by the surface $\vec{S}$, $\vec{v}$ – velocity vector consisting of components [u, v, w] in each of the three orthogonal directions, pn – pressure by the surface dS, $\vec{F}_m$ – it vector of internal forces, cv – specific heat of the gaseous medium at constant volume, T – temperature of gaseous medium, $\dot{q}_n$ – surface density of the heat flux, $\dot{q}_n$ – heat flux density related to the unit mass of the gas.

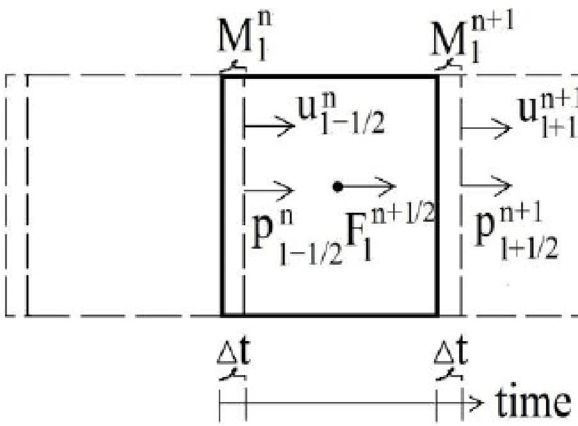

Fig. 1. Diagram of gas flow inside considered finite volume

The system of equations (1) to (3) expresses the gaseous medium flow in the free field region. Solving this system of equations can help present evolution of blast load parameters in time and free-field space and was made using own numerical algorithm (see ref. [9], [10]). Graphical interpretation is presented in Fig. 1. The considered volume of gaseous medium is outlined by thick lines and the adjacent volumes by dotted lines. It is assumed that the two parallel sides are being displaced with velocities Unl-1/2 and Unl+1/2 due to changes in energy. This results in displacement of the mass (M) of gaseous medium to a finite volume, which is highlighted by thick line, and hence the change of density and mass of this volume. Weight increase is associated with a pressure change (p). Consequently, there is also a change in energy. Next, a loop is performed over all finite volumes for the following time steps in order to compute the internal forces. Integration of mentioned equations is made using explicit difference scheme.

The system of equations must be supplemented by the boundary conditions at the interface of building compartments with adjacent finite volumes and at the point of detonation of condensed explosive. When assuming boundary conditions one can simulate the inhibition of gaseous flux by the building compartments. The assumption of the compartment velocity equal to zero (boundary condition) in case of high mass of compartments (concrete, RC) is reasonable, because the blast loading is completed before the compartment deformation started [11]. When considering light compartments (made of steel or glass) a suitable coupling strategy must be chosen. One of the best is the strategy based upon suitable kinematic constraints on the velocities of the fluid and of the structure along the fluid-structure interface.

In the point, when the shock wave region starts, some boundary condition should be known. These are the particle velocity U1/21, the shock wave pressure p1/21, the density of post-explosion gases ρ11 and the temperature of post-explosion gases (see ref. [12]-[14]).

B. Region of Post-Explosion Gases

In case of spherical charge gasses has the shape of a sphere, and in case of cubical charge the shape of an octahedron [15]. In case of a spherical charge, post-explosion gases propagate till 7th time step (2 x 6.5 = 13 – the medium between 10 and 15). Then the density of post-explosion gases is equal to the air density in 7th time step and till this point the shock wave begins to propagate. In case of a cubical charge the region of post-explosion gases finishes in 9th time step. This difference is due to bigger volume of a sphere than an octahedron entered into this sphere. Discrete regions of post-explosion gases in case of spherical charge (till 7th time step) and cubical charge (till 9th time step) are presented in Fig. 2. Boundary conditions in air shock wave region should be equal to the results of calculating parameters in the region of post-explosion gases.

III. COMPARING NUMERICAL RESULTS WITH LITERATURE REPORTS

This paragraph contains checking of correctness of modeling presented in section II. The verification involved comparing calculated blast overpressure distributions in time with measured distributions [16]. Detonations of point charges inside steel and concrete composite structure were analyzed. To validate correctness of three-dimensional solution, blast pressure distribution from a detonation of 1 kg TNT charge in the center point of a vented room was examined [8]. The room was a composite steel and concrete structure of a horizontal square projection with a side of 2.9 m and height 2.7 m (internal dimensions) with a hole in the roof of 1.20 m in diameter (Fig. 3). Authors assumed that elements of the structure and entrances were rigid. 9 pressure gauges were installed on one of the walls (G1 to G9).

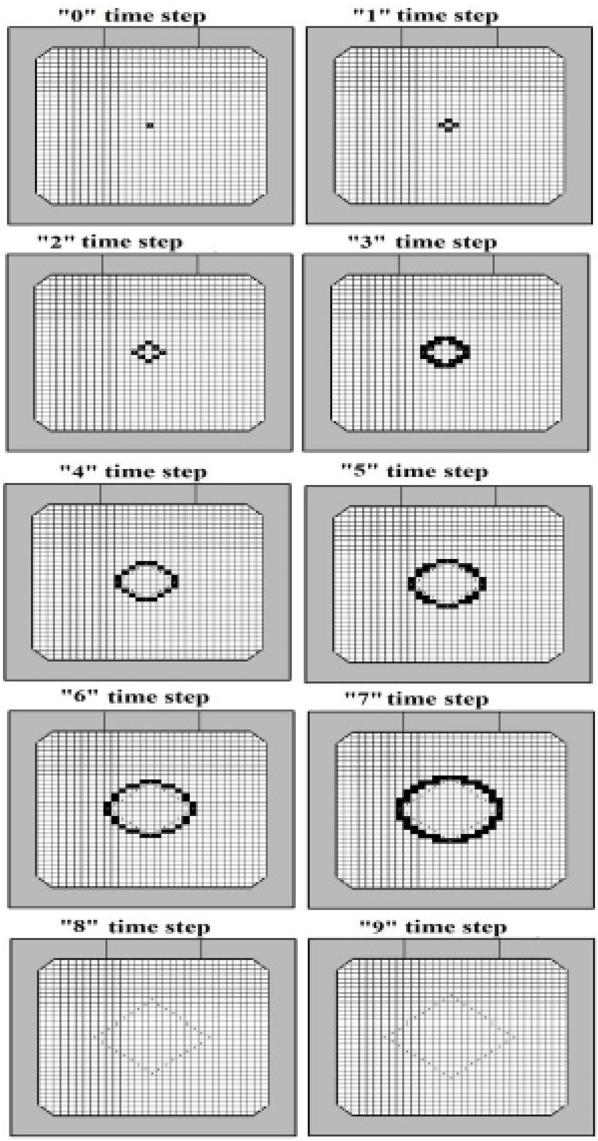

Fig. 2. Discrete spheres(drawn using squares) and octahedrons(drawn using dots) in the following time steps.

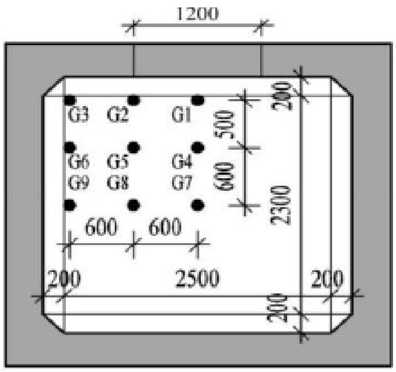

Fig. 3. Test stand scheme

A numerical model was obtained in this case through applying the 3D model of the air shock wave propagation presented in [9], [10]. Internal space of the considered room was divided by cubical finite volumes. Dimension of this volume $\Delta x=\Delta y=\Delta z$ is equal to 0.085 m. The mass velocity of the volumes located next to room`s compartments was assumed for zero in each time step. The mass velocity of side volumes, located next to free-field or in openings, can be of any value. The time step value was assumed for $\Delta t=0.012$ ms.

The cell size should not be bigger than the charge dimension. The compartment velocity is equal to zero because of assuming rigid compartments. The time step value (Δt) is equal to $\Delta x/7000$. This is the time to reach the distance of first cell by the shock wave (the TNT detonation velocity – 7000 m/s). Initial conditions are: the mass velocity U1/21 equal to 690 m/s and the detonation pressure p1/21 equal to 6.7 MPa [10].

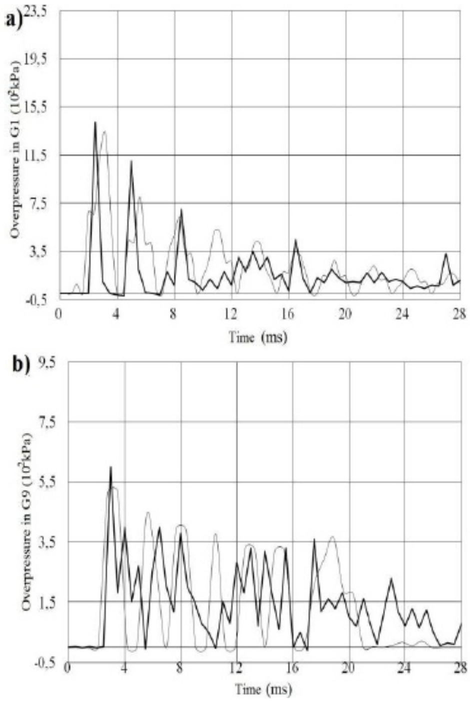

Fig. 4. Overpressure distribution in time: a) in location of gauge G1, b) in location of gauge G9 (thick line – research results; thin line – numerical results).

Fig. 4 presents graphs with an overpressure versus time in gauges G1, and G6. As can be seen, numerical results reflect well the time to reach the shock wave and the duration of the shock wave. It can also be observed that when the overpressure obtained in the tests increases, the overpressure obtained numerically also increases. The same applies to the overpressure decrease. The values of maximum overpressures and impulses (area under the overpressure graph) obtained numerically and those from literature reports are similar.

IV. DYNAMIC RESPONSE OF STRUCTURAL ELEMENT

Present paragraph contains analyses of dynamic response of a structure which was blast loaded. The literature reports provide many different blast load distribution models. This paper considers the exponential and the triangular models [17] and also the model proposed in this article, called later as realistic. Simplified methods of blast load estimation inside vented or unvented room rely mainly on using empirical equations [17].

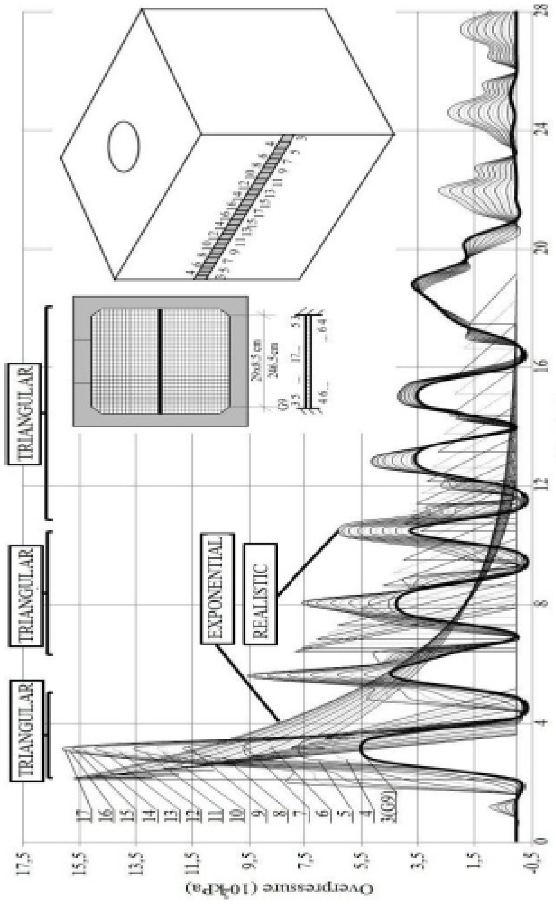

Fig. 5. a) overpressure distribution in time in points 3÷17 for exponential, triangular and realistic model; b) room cross-section i c) axonometric projection of room with hatched isolated beam and points 3÷17

Assessment of previously mentioned blast load models was made using comparison of deflection change in time when considering the isolated structural element. Nowadays this is common approach because within maximum peak deflection one can easily find the residua deflection. Deflection analysis was prepared using overpressure distribution in time inside considered room.

As a result of presented modeling air shock wave parameters can be obtained in each finite volume inside considered room (fig. 5). Figure 5 presents isolated part of the wall which was divided by 33 cells and the overpressure distributions (for three kinds of models) are presented for each cell, strictly for 15 cells in locations 3÷17 because of symmetry (fig. 5a).

In second step, dynamic response of isolated structural beam element was made. The location of the beam and its scheme are presented in fig. 5b and 5c, respectively. It was assumed that the supports are fixed, length is equal to 2.465 m, width of cross-section is equal to 8.5 cm, height 19 cm (including: steel plate, thickness 1 cm; concrete, thickness 17 cm; steel plate, thickness 1 cm), fyk=235 MPa, ES=210 GPa, fck=25MPa, Ec=31 GPa. The damping also was taken into consideration, characterized using modified friction damper equal to 0.25. Free vibration period is equal to 0.0097 s.

The dynamic analyses were made using Finite Difference Scheme and integration of dynamic differential equations of Bernoulli beam. The model of a beam is characterized using system of discrete mass located along longitudinal beam axis in nodes offset equal to Δx.

The equation of motion in i-th node can be written as:

$$P_i^n + Q_i^n - Q_{i-1}^n - B_i^n - S_{c,i}^n = 0, \qquad (4)$$

where: P_i^n – force determined by multiplying the overpressure value by beam width and Δx value, Q_i^n, Q_{i-1}^n – transverse forces, $B^n = \Delta m_i \ddot{w}$ – inertia force, $S_{c,i}^n = c\,w$ – damping force, Δm – discrete mass, w – node deflection, c – friction damper. Equation of motion were integrated using Finite Difference Scheme in time. The curvature in i-th node can be calculated as:

$$k_i^n = \left(w_{i-1}^n - 2w_i^n + w_{i+1}^n\right)/\Delta x^2. \qquad (5)$$

The moment-curvature physical law was used so the bending moment can be written as:

$$M_i^n = k_i^n B_c, \qquad (6)$$

where Bc – bending stiffness of beam cross-section.

Transverse force can be calculated using condition of bending moments balance against i-th node:

$$Q_i^n = \left(M_{i+1}^n - M_i^n\right)/\Delta x. \qquad (7)$$

Graphs of deflections change in time are presented in Fig. 6. Beam vibrations with considering damping are presented using thick lines and vibrations without considering damping are presented using dotted lines. Maximum deflections influenced realistic model of overpressure are about 30% less than deflections influenced exponential model, however the impulse applied in case of realistic overpressure is 200% bigger than in case of exponential overpressure. Maximum deflections influenced triangular model of overpressure are about 50% less than deflections influenced realistic model, however the impulse applied in case of triangular overpressure is 400% less than in case of realistic overpressure. This is a result of applying further overpressure impulses to the beam when it comes back to the location before deformation. This provides velocity reduction of deformed beam.

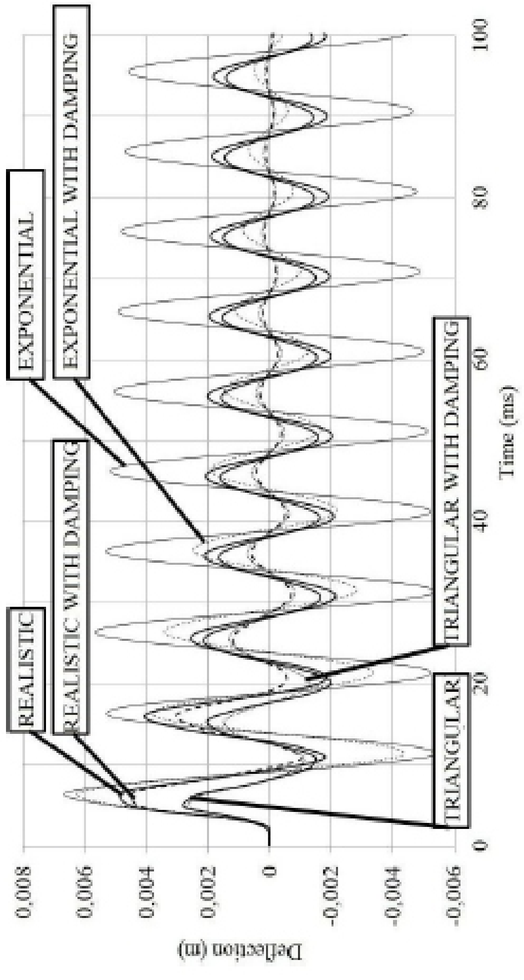

Fig. 6. Change of deflection in time in dependents from blast load distribution model

This work was supported by grant RMN No 800/2016 funded by Faculty of Civil Engineering and Geodesy in Military University of Technology.

REFERENCES

[1] A. Zare, M. Janghorban, "Shock factor investigation in a 3-D finite element model under shock loading," Lat. Am. J. Solids Struct., vol. 10, pp. 941-952, January 2013.

[2] Z. M. Jaini, Y. T. Feng, D. R. J. Owen, S. N. Mokhtar, "Fracture Failure of Reinforced Concrete Slabs Subjected to Blast Loading Using the Combined Finite-Discrete Element Method," Lat. Am. J. Solids Struct., vol. 13, pp. 1086-1106, February 2016.

[3] H. R. Tavakoli, F. Kiakojouri, "Numerical dynamic analysis of stiffened plates under blast loading," Lat. Am. J. Solids Struct., vol. 11, pp. 185-199, January 2014.

[4] J. Siwiński, A. Stolarski, "Analysis of the external explosion action on the building barriers," Bulletin MUT, vol. 64, no. 2, pp. 173-196, June 2015. (in Polish)

[5] M. Lidner, "Numerical Calculation of a Blast Load on the Example of a Slab and Wall Structure of any Geometry (Published Conference Proceedings style)," in Proc. 5th Intl Worksh. Performance, Protection & Strengthening of Structures Under Extreme Loading, East Lansing, 2015, pp. 563–570.

[6] M. Lidner, Z. Szcześniak, "Numerical Calculation of a Blast Load," Logistyka, no. 4, pp. 9397-9403, September 2015. (in Polish)

[7] M. Lidner, Z. Szcześniak, "Simplified Numerical Modelling of a Blast Load Impact," Appl. Mech. Mater., vol. 797, pp. 131-136, November 2015.

[8] F. Casadei, N. Leconte, "Coupling finite elements and finite volumes by Lagrange multipliers for explicite dynamic fluid-structure interaction," Int. J. Numer. Methods Eng., vol. 86, no. 1, pp. 1-17, April 2011.

[9] M. Lidner, Z. Szcześniak, "Numerical Analysis of Blast Load from Explosive Materials Using Finite Volume Method," Key Eng. Mat., vol. 723, pp. 789-794, January 2017.

[10] M. Lidner, Z. Szcześniak, "Blast load estimation using Finite Volume Method and linear heat transfer," MATEC Web Conf., vol. 86, 01027, December 2016.

[11] V. T. Nguyen, B. A. Gatzhammer, "Fluid structure interactions partitioned approach for simulations of explosive impacts on deformable structures," Int. J. Impact Eng., vol. 80, pp. 65-75, February 2015.

[12] L. Mazurkiewicz, J. Malachowski, P. Baranowski, "Blast loading influence on load carrying capacity of I-column," Eng. Struct., vol. 104, pp. 107-115, December 2015.

[13] A. Erdik, S. A. Kilic, N. Kilic, S. Bedir, "Numerical simulation of armored vehicles subjected to undercarriage landmine blast," Shock Waves, vol. 26, pp. 449-464, May 2015.

[14] B. Yan, F. Liu, D. Y. Song, Z. Jiang, "Numerical study on damage mechanism of RC beams under close-in blast loading," Eng. Fail. Anal., vol. 51, pp. 9-19, March 2015.

[15] E. Włodarczyk, "Mechanical impact of point explosion on the walls and ceiling of object," Bulletin MUT, vol. 39, no. 11, pp. 131-153, November 1980. (in Polish)

[16] V. R. Feldgun, Y. S. Karinski, D. Z. Yankelevsky, "A simplified model with lumped parameters for explosion venting simulation," Int. J. Impact Eng., vol. 38, no. 12, pp. 964-975, December 2011.

[17] J. Siwiński, A. Stolarski, "Analysis of the internal explosion affecting building barriers," Bulletin MUT, vol. 64, no. 2, pp. 197-211, June 2015. (in Polish)

Instructions for Authors

Essentials for Publishing in this Journal

1 Submitted articles should not have been previously published or be currently under consideration for publication elsewhere.

2 Conference papers may only be submitted if the paper has been completely re-written (taken to mean more than 50%) and the author has cleared any necessary permission with the copyright owner if it has been previously copyrighted.

3 All our articles are refereed through a double-blind process.

4 All authors must declare they have read and agreed to the content of the submitted article and must sign a declaration correspond to the originality of the article.

Submission Process

All articles for this journal must be submitted using our online submissions system. http://enrichedpub.com/ . Please use the Submit Your Article link in the Author Service area.

Manuscript Guidelines

The instructions to authors about the article preparation for publication in the Manuscripts are submitted online, through the e-Ur (Electronic editing) system, developed by **Enriched Publications Pvt. Ltd**. The article should contain the abstract with keywords, introduction, body, conclusion, references and the summary in English language (without heading and subheading enumeration). The article length should not exceed 16 pages of A4 paper format.

Title

The title should be informative. It is in both Journal's and author's best interest to use terms suitable. For indexing and word search. If there are no such terms in the title, the author is strongly advised to add a subtitle. The title should be given in English as well. The titles precede the abstract and the summary in an appropriate language.

Letterhead Title

The letterhead title is given at a top of each page for easier identification of article copies in an Electronic form in particular. It contains the author's surname and first name initial .article title, journal title and collation (year, volume, and issue, first and last page). The journal and article titles can be given in a shortened form.

Author's Name

Full name(s) of author(s) should be used. It is advisable to give the middle initial. Names are given in their original form.

Contact Details

The postal address or the e-mail address of the author (usually of the first one if there are more Authors) is given in the footnote at the bottom of the first page.

Type of Articles

Classification of articles is a duty of the editorial staff and is of special importance. Referees and the members of the editorial staff, or section editors, can propose a category, but the editor-in-chief has the sole responsibility for their classification. Journal articles are classified as follows:

Scientific articles:

1. Original scientific paper (giving the previously unpublished results of the author's own research based on management methods).

2. Survey paper (giving an original, detailed and critical view of a research problem or an area to which the author has made a contribution visible through his self-citation);

3. Short or preliminary communication (original management paper of full format but of a smaller extent or of a preliminary character);

4. Scientific critique or forum (discussion on a particular scientific topic, based exclusively on management argumentation) and commentaries. Exceptionally, in particular areas, a scientific paper in the Journal can be in a form of a monograph or a critical edition of scientific data (historical, archival, lexicographic, bibliographic, data survey, etc.) which were unknown or hardly accessible for scientific research.

Professional articles:

1. Professional paper (contribution offering experience useful for improvement of professional practice but not necessarily based on scientific methods);
2. Informative contribution (editorial, commentary, etc.);
3. Review (of a book, software, case study, scientific event, etc.)

Language

The article should be in English. The grammar and style of the article should be of good quality. The systematized text should be without abbreviations (except standard ones). All measurements must be in SI units. The sequence of formulae is denoted in Arabic numerals in parentheses on the right-hand side.

Abstract and Summary

An abstract is a concise informative presentation of the article content for fast and accurate Evaluation of its relevance. It is both in the Editorial Office's and the author's best interest for an abstract to contain terms often used for indexing and article search. The abstract describes the purpose of the study and the methods, outlines the findings and state the conclusions. A 100- to 250-Word abstract should be placed between the title and the keywords with the body text to follow. Besides an abstract are advised to have a summary in English, at the end of the article, after the Reference list. The summary should be structured and long up to 1/10 of the article length (it is more extensive than the abstract).

Keywords

Keywords are terms or phrases showing adequately the article content for indexing and search purposes. They should be allocated heaving in mind widely accepted international sources (index, dictionary or thesaurus), such as the Web of Science keyword list for science in general. The higher their usage frequency is the better. Up to 10 keywords immediately follow the abstract and the summary, in respective languages.

Acknowledgements

The name and the number of the project or programmed within which the article was realized is given in a separate note at the bottom of the first page together with the name of the institution which financially supported the project or programmed.

Tables and Illustrations

All the captions should be in the original language as well as in English, together with the texts in illustrations if possible. Tables are typed in the same style as the text and are denoted by numerals at the top. Photographs and drawings, placed appropriately in the text, should be clear, precise and suitable for reproduction. Drawings should be created in Word or Corel.

Citation in the Text

Citation in the text must be uniform. When citing references in the text, use the reference number set in square brackets from the Reference list at the end of the article.

Footnotes

Footnotes are given at the bottom of the page with the text they refer to. They can contain less relevant details, additional explanations or used sources (e.g. scientific material, manuals). They cannot replace the cited literature.
The article should be accompanied with a cover letter with the information about the author(s): surname, middle initial, first name, and citizen personal number, rank, title, e-mail address, and affiliation address, home address including municipality, phone number in the office and at home (or a mobile phone number). The cover letter should state the type of the article and tell which illustrations are original and which are not.

Address of the Editorial Office:

Enriched Publications Pvt. Ltd.
S-9, IInd FLOOR, MLU POCKET,
MANISH ABHINAV PLAZA-II, ABOVE FEDERAL BANK,
PLOT NO-5, SECTOR -5, DWARKA, NEW DELHI, INDIA-110075,
PHONE: - + (91)-(11)-45525005